Performance analysis of a PEGylation process

Process comparison of a tubular reactor with recirculation to a conventional batch reactor

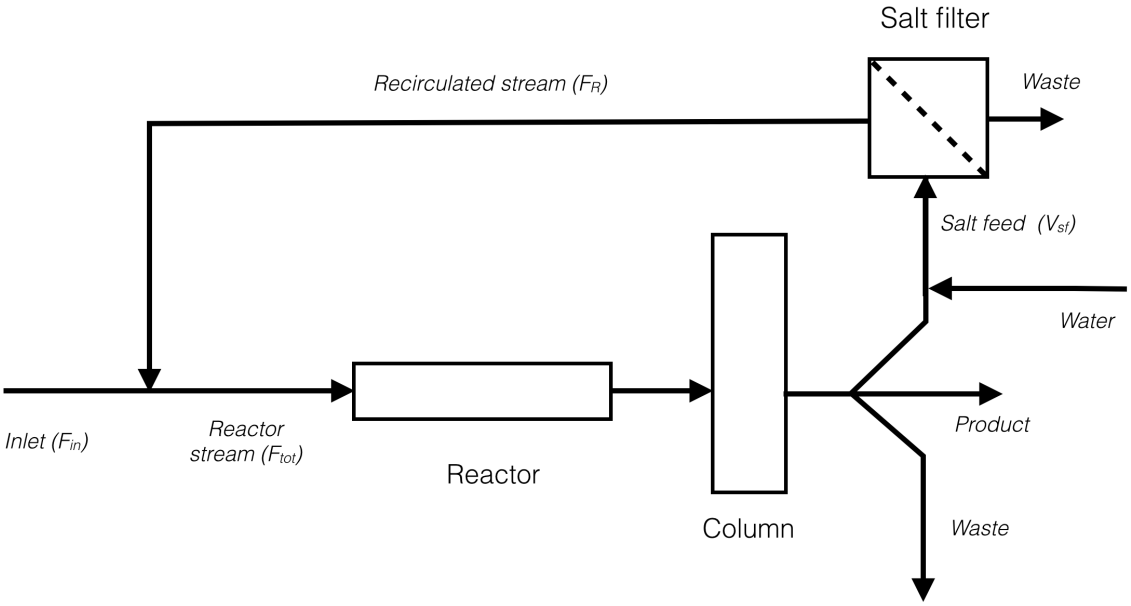

Boris Torbica

Department of Chemical Engineering
Master Thesis 2015

LUND UNIVERSITY

Performance analysis of a PEGylation process

Process comparison of a tubular reactor with recirculation to a conventional batch reactor

by

Boris Torbica

Department of Chemical Engineering
Lund University

September 2015

Supervisor: **PhD NiklasAndersson**
Examiner: **Professor Bernt Nilsson**

Postal address
P.O. Box 124
SE-221 00 Lund, Sweden
Web address
www.chemeng.lth.se

Visiting address
Getingevägen 60

Telephone
+46 46-222 82 85
+46 46-222 00 00
Telefax
+46 46-222 45 26

Acknowledgements

I would first like to express my gratitude to Professor Bernt Nilsson for having presented me with the opportunity to work on my master thesis at the Department of Chemical Engineering, Lund University. Thank you for the advices and the good knowledge I gained during my time here.

Furthermore, I would also like to give an enormous thank to my supervisor, PhD Niklas Andersson. I would have never made through this project if it was not for all the support, help and great knowledge. Thank you for your time and patience.

A special thanks goes to Erik Bergman for fixing the illustrative pictures for the theory part of this project. I would also like to thank Fredrik Tegnér for providing me with experimental data.

Very special thanks to André Holmberg PhD Student, MSc in Chemical Engineering, fellow deadlifter and friend for his technical expertise, motivation and moral support. Thank you also for all the interesting conversations!

I would like to express deep gratitude to my parents and my brother for always being there for me. You all mean the world to me.

I humbly thank my dear friend Dr. Johan Johansson for always being there for me. I never would have come this far if it would not have been for you. I would also like to give special thanks to my friends David Dahlgren, Kajsa Nilsson, Axel Forsberg and Erik Bergman for helping me through difficult times. And of course a big thank to all my friends for being supportive and making my time here in Lund enjoyable!

Lund
September 2015

Boris Torbica

Abstract

Since the rise of therapeutical proteins, there has been a growing interest in biopharmaceuticals over the years. Research was made to combat various protein weaknesses like fast degradation and low solubility. A discovery in the 1970s suggested that an attachment of polyethylene glycol (PEG) on protein surfaces would solve the specific problems. Today this process is known as PEGylation and is widely used in biopharmaceutical industry.

Because of strict pharmaceutical regulations, the PEGylation process is currently performed in batch reactors. These in turn are often connected to Ion Exchange Chromatography (IEC) as a purification step after reaction. However, this type of PEGylation process set-up is not so efficient. Major losses are made due to batch being a non-continuous process and not recirculating unreacted biopharmaceuticals. One suggestion to improve the process is by implementing a tubular reactor system and a recirculation stream.

Models were created, one for a batch system and one for the tubular system. Sensitivity analyses were made for every part in the systems to enhance production. Cases were made for each system and then weighed against each other. After selecting best case for each process schematic, the two processes were then compared to each other.

The results show a clear improvement of the tubular schematics compared to the batch schematics. Productivity was increased by 71%, from 0.0126 to 0.0216 $g \cdot h^{-1}$. The product system yield of was increased by 11%, from 0.43 to 0.46. Waste formation was able to be reduced by 42%, from 0.25 to 0.15. These numbers show a clear potential for tubular reactor systems implemented with recirculation.

PEGyleringsprocess på löpande band

Nytänk ska rädda värdefullt läkemedel

Uppkomsten av läkemedelsproteiner har haft betydelsefull påverkan på läkemedelsindustrin. Så kallad PEGylering är en vanlig efterbehandling av dessa proteiner. Idag kännetecknas PEGylering av en stillastående process som är tidsödande med stora förluster. Kan man med nytänk ämnas lösa dessa problem?

Tillverkningsprocessen och användningen av terapeutiska (läkande) proteiner har varit relativt framgångsrik. Och med genteknikens framsteg ökar intresset allt mer för nyttjandet av dessa proteiner. Dock har användningen inte alltid varit problemfri. Första problemet som upptäcktes var att läkemedelsproteinerna lätt bröts ner. Med hjälp av ett speciellt ämne som kallas för **P**oly**E**tylene**G**lykol (**PEG**) kunde detta problem åtgärdas. PEG består främst av kol-atmomer i kedjor som man binder in på ett läkemedelsprotein i en process som kallas för PEGylering. Kedjan agerar då som ett tillfälligt skydd från yttre påverkan för proteinet. Dessa PEG-kedjor går att fästa på flera olika ställen på proteinet beroende på hur många speciella platser som finns tillgängliga.

På grund av hårda regleringar i läkemedelsbranschen utförs PEGylering idag för enkelhetens skull i stora kärl, kallade batch-reaktorer. Detta är en stillastående process. Processen går till på det viset att man blandar ihop läkemedlet, PEG:en och andra kemikalier som behövs för PEGyleringsprocessen och låter dessa reagera. Efter att reaktionen pågått i en viss tid stoppas reaktionen och den önskade produkten renas upp ur blandningen. I snitt hinner 40% av proteinen PEGyleras till den grad man vill åstadkomma innan alltför många biprodukter bildas. Däremot går det åt en hel del tid till att rengöra reaktorn efter användning och annat arbete vid hanteringen av utrustningen. Detta är vad man kallar för spilltid som annars hade kunnat utnyttjats för reaktion.

Idag arbetas det därför med att utveckla nya metoder på att försöka snabba på processen och förhindra förluster. Ett nytt och mer hållbart förslag att hantera läkemedelsbehandlingen är att gå över till en rörlig process. Med rörlig process menas att man pumpar läkemedlet med PEG och resterande ingredienser och låter dem reagera medan de färdas i ett rör, en så kallad tubreaktor. Med detta maskineri kan man avbryta processen tidigare och med lättare möjligheter även återvinna icke-PEGylerat läkemedel. Tack vare detta slipper man slänga icke-PEGylerat läkemedel. Simuleringsresultat visade att man kunde minska reaktionstiden och ändå öka utbytet med 11 % av produkten samt öka produktionshastigheten med hela 71 %. Samtidigt minskades utbytet av biprodukter med 42 %.

Det lyckade försöket att simulera PEGylering i en tubreaktor visar stora möjligheter i att effektivisera läkemedelsprocessen. Flera designmöjligheter öppnas upp som tidigare inte var genomförbara. Med detta system kan man både spara in tid och samtidigt rädda läkemedel som annars kasserats.

En hel del arbete kvarstår. Eftersom det rör sig om läkemedel måste fler simuleringar och experiment utföras. Många faktorer som måste tas hänsyn till innan detta kan användas i industrin. Mer hållbar och framförallt säker teknik måste tas fram innan det kan godkännas för bruk. Däremot pågår det en hel del forskning kring detta område och resultaten som visat verkar lovande!

Table Of Contents

1 Introduction

1.1 Background

Since the advancement of therapeutical proteins and genetic engineering, there has been a steady increase in interest of therapeutical proteins. However, being able to make use of these proteins has not been without difficulties. Major weaknesses were shown regarding pharmacokinetic properties such as low solubility, instability with as well as rapid enzymatic degradation of the proteins in the human body (1,2,3). Two major studies presented in the 1970's by a research team under Professor Frank F. Davis, at Rutgers University provided a promising solution to the lack of pharmacokinetic characteristics. The researcher team chose to covalently attach polyethylene glycol (PEG) to bovine liver catalase and bovine serum albumin in a reaction process now known as PEGylation. Studies performed *in vivo* with these PEGylated components indicated no immune response towards the PEGylated enzymes, less enzymatic degradation activity, higher solubility and exhibited an increase in half-life in the blood stream (4,5,6,7). Since then, countless PEGylated pharmaceutical proteins have been approved by the FDA. As of now they make up a large part of the medicinal industry and their role keeps increasing by being a relatively inexpensive source for improving the properties of biopharmaceuticals (8,6,9,10).

The main challenge today is making the PEGylation process efficient because of the costly production of biopharmaceuticals. There action operation is ordinarily carried out in rather small batch reactors, since they are easy to maintain and control. After PEGylation, the downstream processing is usually performed with an Ion Exchange Chromatography (IEC). The whole procedure often returns relatively low productivity and yields. Continuous processes on an industrial scale are generally considered more profitable than running batch reactors. It is therefore a matter of interest to investigate this matter further (1).

1.2 Aim

This study will first and foremost focus on evaluating the possibility of recreating experimental batch reactor conditions by simulations of batch and tubular reactors in Matlab. Then efforts are made to simulate complete process systems by first implementing an IEC column to each reactor. An attempt will be made to apply recirculation in the tubular reactor format after the IEC separation. This will be scrutinised in order to try and increase the PEGylation yield of biopharmaceutical protein and thus also adding a salt filter to the system to handle the salt concentrations from the IEC column before recirculating back.

Sensitivity analyses are also intended to be studied of both the salt filter and the IEC column to increase the efficiency of the tubular schematics. Next step will then be to try and optimise the tubular reactor itself. The aim is to evaluate the process performance of the tubular reactor by studying different approaches to the tubular schematics.

In the end both batch and tubular process performances of each system will be compared. The product target in the simulations is considered to be monoPEGylated lysozyme whereas native lysozyme is recirculated. The comparison will mainly be focused on comparing yield and productivity of the two different methods.

2 Theory

2.1 Polyethylene glycol

Polyethylene glycol (PEG) is a polymer constructed by linking ethylene glycol into chains. The structure of PEG comes in both linear and branched forms with different molecular weights (MW) depending on final desired properties. The linear PEG molecule, H-$(OCH_2CH_2)_n$-OH, is an example of a simple and well known chain with *n* number of ethylene glycol components attached together, see Figure 2.1 (11,7). A distinctive feature of PEG is its nature of being soluble in both organic and aqueous solvents. It is estimated that the oxygen of the glycol interacts with up to seven water molecules. This swells the polymer several times more compared to molecules of similar MW and increases the hydrodynamic radius (1,6,12).

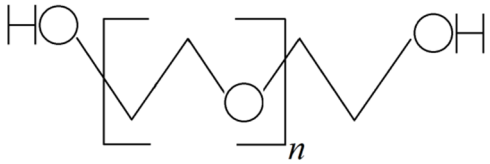

Figure 2.1. Linear PEG molecule with n number of ethylene glycols attached in a chain. Picture made by author.

PEGs are of interest in the biopharmaceutical industry as they are used in a reaction process called PEGylation for improving pharmacokinetic properties of biopharmaceutical components (11,7). Studies show several benefits of PEGylation, one of which is an improvement *in vivo* half-life and shelf-life. One major benefit of a better half-life is that same potency can be achieved with smaller dosage of the drug (1,8,11). Therefore, fewer injections are required for the patients thus making more of the therapeuticals available as well as reducing the risk of infections. The number of PEG-chains bound to biomolecules is a major factor affecting the degree of improvement regarding half-life. Observations show that degradation of PEGylated biomolecules takes longer as the number of attached PEG-chains increases. Even positional isoforms tend to differ pharmacokinetically (1,3,6,7). Protein activity is also affected due to steric hindrance and for that reason it is desirable to achieve site-specific PEGylation (9,13).

2.1.1 Reaction models

Numerous types of PEGylation strategies have been developed through the years. These reactions are often complex processes and depend on the structure forms of PEG molecules and polypeptides (9,7).

For long, PEGylation reactions have been non-specific site reactions. Usually, PEGylation strategies are general and therefore give rise to chemical divergences. This is especially a problem when it comes to small biomolecules in relation to large polymers. However, site-specific PEGylations can be achieved by targeting structural functional groups like N-terminus(α-amines) and lysine side chains(ϵ-amines) (14).

Lysozyme is a well-known protein in PEGylation studies with its three amino-terminuses exposed. The three amino-terminuses enable the lysozyme to be PEGylated three times with multi-pronged reaction mechanisms as illustrated in Figure 2.2 below.

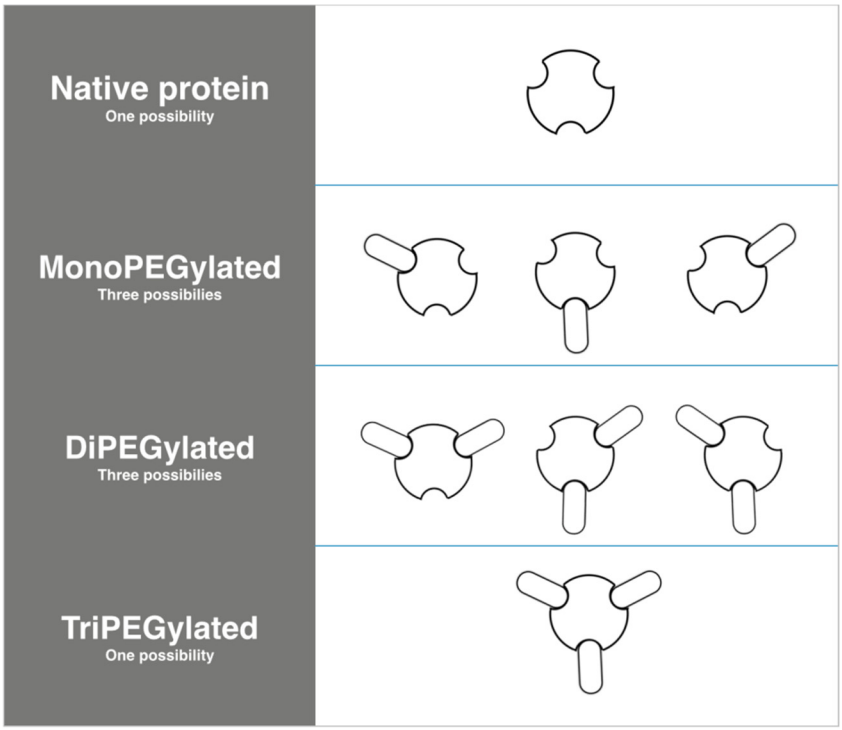

Figure 2.2. Illustration of all different site combinations of PEGylation for lysozyme.

One method describes a reaction mechanism where mPEG-aldehyde is used to conjugate with lysozyme using sodium cyanoborohydride as reducing agent, see Figure 2.3. (15).

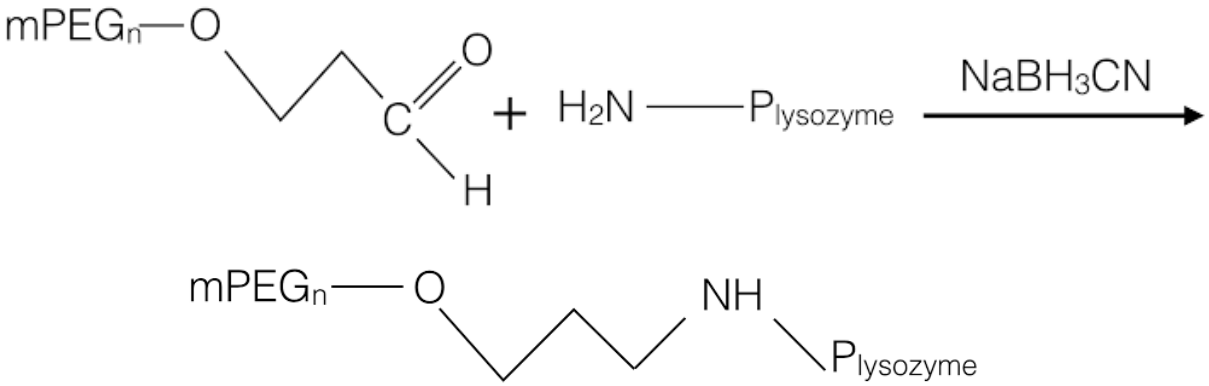

Figure 2.3. Illustration of an n long mPEG-aldehyde chain reacting with a protein (P), lysozyme in this case, by using sodium cyanoborohydride as a reducing agent.

It should also be known that the reaction described in Figure 2.3 is dependent on a deactivation reaction of PEG by $NaBH_3CN$ (CBH) (16).

2.2 Reaction phase

Through the years, numerous different reactors have been tested to achieve optimal PEGylation conditions. This paragraph will present two models, one of which is used today and one which is considered for a continuous process.

2.2.1 Batch reactor

PEGylation is today mainly performed by using batch reactors (17). The main reason for this can be traced to regulatory practices in the pharmaceutical industry. Strict regulations require traceability from the final product all the way back to the sources for each process. End products must also be able to show that they have gone through the exact same process. These reasons are often enough for industries to apply batch reactors as their first choice (18).

Several advantages also come with batch reactors. They are simple to operate and have relatively easy maintenance requirements. Further, conditions provided by a batch reactor are ideal for site-specific PEGylation if this is desired. However, one major disadvantage concerning PEGylation processes in batch reactors is that the product residence time in the vessel is usually unflavoured and therefore continues to react, forming undesirable by-products (18). As known, this reactor type runs discontinuously and therefore dead time is needed to be taken into consideration (19).

The mass balance for a typical batch reactor with assumed constant volume can be expressed by the ordinary differential equation; see Equation (1).

$$r_i = \frac{dc_i}{dt} \tag{1}$$

Where r_i is the rate of reaction for component i and equal to the concentration difference of the component (dc_i) through the reaction time (dt) (19).

2.2.2 Tubular reactor

Tubular reactors are often suggested as a way of making a process continuous. It can be run non-stop for long periods without having to break the process for maintenance. Dead time is therefore negligible in comparison to the batch reactor. The reactor type is easy to adjust and optimise for a certain process. Compared to the batch reactor the residence time is more adjustable since it depends on the tube length and the flow velocity through the tube. However, pressure drop increases with longer tubes. Continuous flow rates offer high volumes for reactions with possibility to be directly connected to chromatographic systems. Start-ups and shut downs are generally neglected and the tube is therefore considered to be time-effective (20,19).

A stationary ideal tube reactor is usually expressed as an ordinary differential equation as seen in Equation (2) below.

$$dF_i = r_i dV \tag{2}$$

Where dF_i is the flow difference between the outlet and the inlet of the tube and r_i being the rate of reaction multiplied to the reactor volume (dV) (19).

2.3 Purification phase

Modification of polypeptides presents transformed states of size, surface charges and hydrophobicity. These altered states enable various purification possibilities. This paragraph will present two dominating purification approaches in the PEGylation process (18).

2.3.1 Ion Exchange Chromatography

Ion Exchange Chromatography (IEC) has long been considered to be the most reliable type of chromatography for purification in PEGylation processes. The purification mechanism of IEC is based on the interaction of component surface charges and isoelectric point (pI) with IEC media, as illustrated in Figure 2.4 (18).

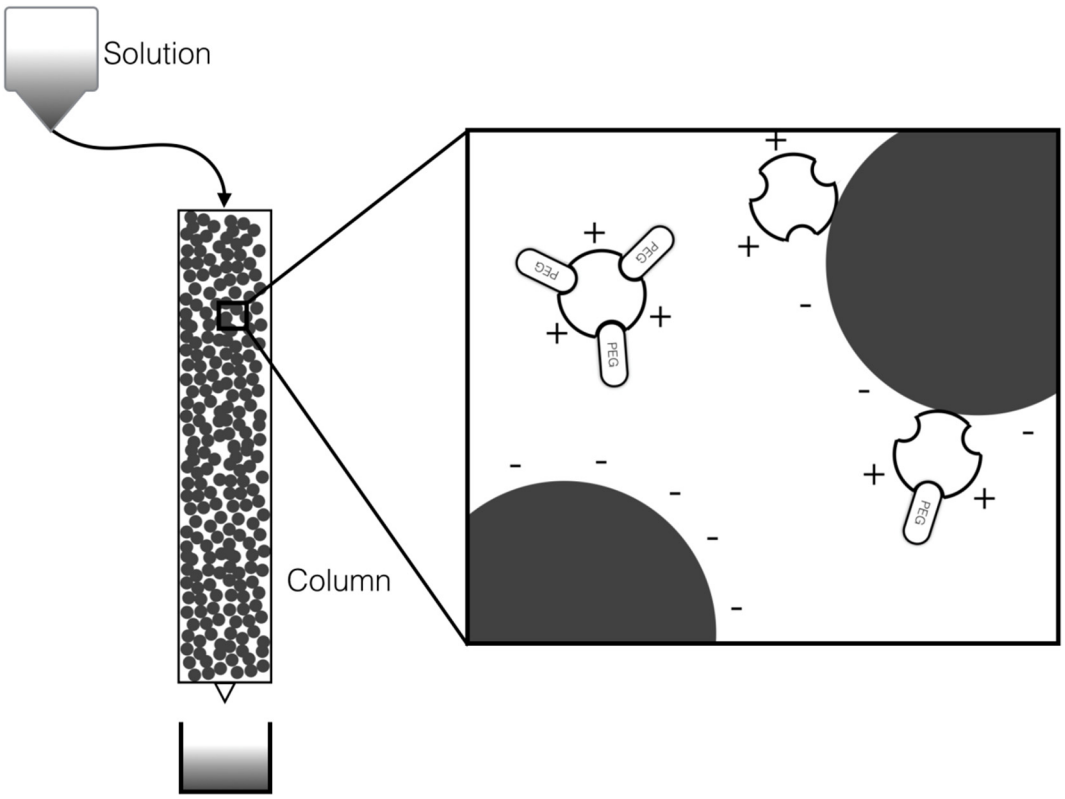

Figure 2.4. Depicting a typical cation exchange chromatography column where a non-PEGylated and a monoPEGylated protein are attached to a negatively charged bead.

Abundance of surface charges depends on two main factors. The first factor relates to isoforms that experience varied shielding effects due to PEGylation of different active sites. The second factor relates to the degree of PEGylation. A highly PEGylated polypeptide will have less of its surface charges exposed and thus weaker interactions with the IEC media. Consequently the retention time will increase with decreased number of attached PEG-chains as the eluent gradient is raised during elution. This also means that native proteins will have the longest retention time since they have the strongest possible interactions (1,9,13).

As with every technology, there are pros and cons by using it. The main advantage of IEC is that it allows for high-flow continuous processes (21). Recent studies have even shown successful separations of isoforms by a pH-regulated gradient (9,13). A disadvantage to consider when dealing with IEC, is that the outlet feed needs to be diluted several times because of the

high salt concentration following the elution process. Another disadvantage to note is the fouling issue which builds up because of the salt (18).

Desalting
Removal of buffer salts from a feed is sometimes preferred for various reasons. A well-established method for this purpose is the diafiltration system and has been the choice for industrial processes for a long time. It has been the choice of the industry since a well-designed diafiltration system can be time efficient and be used for continuous processes. Desalting by diafiltration is performed by membranes where only molecules of a particular size can pass the membrane barrier (22).

Continuous separation
It is overall more cost-effective to manage a continuous process than a batch in large-scale productions. The simulated moving bed (SMB) is one example of a continuous purification model. This setup often generates high purities and yields decreased solvent consumption. SMB processes are also known for being able to handle separations with somewhat bad resolutions and nevertheless provide excellent results, even regarding separation of isoforms (1,23).

2.3.2 Size Exclusion Chromatography
As stated earlier the hydrodynamic radius of a biomolecule increases as it gets more PEGylated. For that reason, separation can be achieved with the Size Exclusion Chromatography (SEC). One of the most efficient features of SEC is separation of components with low molecular weight. In general, the elution order in a SEC follows the degree of PEGylation, where largest molecules come out first. Good resolutions for preparative scale productions are generally achieved according to a rule of thumb where the molecular weight of PEGylated proteins differs by a factor of two (1,9,18). Research has also shown that it becomes increasingly difficult to achieve a good resolution for multi-PEGylated proteins (2).

The method is relatively simple, cost-effective and well established (8,18). Though, it is worth noting that SEC is not reliable when separating for a preparative scale. Satisfying purity goals may not always be attained with a SEC column alone and is therefore typically connected with an IEC as a polishing step. SEC is also unable to separate isoforms IEC is able to (1,13).

3 Methods

This paragraph will include the methods that were applied for the simulations as well as assumptions for the presented models. Nomenclature for the used equations can be viewed in paragraph **8**.

3.1 Reaction model

This subparagraph first presents the general reaction model and then the models adopting it. Simulations were based on an experimental PEGylation study of PEG-aldehyde in a batch reactor with sodium cyanoborohydride as a reducing agent, see Table 3.1 for relevant experimental values. MonoPEGylated lysozyme was regarded as the desired product.

Table 3.1. Experimental values used for the simulation. (16)

PEGMW ($g \cdot mole^{-1}$)	c_{lys} ($mg \cdot mL^{-1}$)	PEG/Lys-ratio (-)	$NaBH_3CN$ ($mg \cdot mL^{-1}$)	Reaction time (h)
5000	7.5	8/1	40	3

3.1.1 General reaction

The general reaction model is described by Reactions [1-4] and was given by Figure 2.3. For this project, lysozyme is thought to reach tri-PEGylated state. It was assumed that all three monoPEGylated forms were desired products.

$$Lysozyme + PEG \xrightarrow{NaBH_3CN} MonoPEG \quad [1]$$

$$MonoPEG + PEG \xrightarrow{NaBH_3CN} DiPEG \quad [2]$$

$$DiPEG + PEG \xrightarrow{NaBH_3CN} TriPEG \quad [3]$$

$$PEG \xrightarrow{NaBH_3CN} PEG^* \quad [4]$$

Reaction [4] defines the elimination process of PEG-chains by sodium cyanoborohydride. Each reaction in [1-4] is described by first order irreversible rate of reaction terms (r_j) in Equations (3-6) respectively. As stated by Tegnér (2015), the reactions are dependent on the presence of sodium cyanoborohydride and for this reason, $NaBH_3CN$ is included in Equations (3-6).

$$r_1 = k_1 \cdot c_{PEG} \cdot c_{CBH} \cdot c_{lys} \quad (3)$$

$$r_2 = k_2 \cdot c_{PEG} \cdot c_{CBH} \cdot c_{mono} \quad (4)$$

$$r_3 = k_3 \cdot c_{PEG} \cdot c_{CBH} \cdot c_{di} \quad (5)$$

$$r_4 = k_4 \cdot c_{PEG} \cdot c_{CBH} \quad (6)$$

The kinetic reaction constants (k_j) in Equations (3-6), were retrieved from a batch experimental setup by Tegnér (2015), see Table 3.2.

Table 3.2. The kinetic reaction coefficients used for the simulation.

Reaction coefficient	Value
$\mathbf{k_1}$	5.74 $dm^6 \cdot mole^{-2} \cdot s^{-1}$
$\mathbf{k_2}$	3.96 $dm^6 \cdot mole^{-2} \cdot s^{-1}$
$\mathbf{k_3}$	3.47 $dm^6 \cdot mole^{-2} \cdot s^{-1}$
$\mathbf{k_4}$	0.0282 $dm^3 \cdot mole^{-1} \cdot s^{-1}$

3.1.2 The batch reactor

A general mass balance of a batch reactor was set for each component according to Equation (1) with reaction rate terms as expressed by Equations (3-6), see Equations (7-12).

$$\frac{\partial c_{lys}}{\partial t} = -r_1 \tag{7}$$

$$\frac{\partial c_{mono}}{\partial t} = r_1 - r_2 \tag{8}$$

$$\frac{\partial c_{di}}{\partial t} = r_2 - r_3 \tag{9}$$

$$\frac{\partial c_{tri}}{\partial t} = r_3 \tag{10}$$

$$\frac{\partial c_{CBH}}{\partial t} = -\sum_{j=1}^{4} r_j \tag{11}$$

$$\frac{\partial c_{PEG}}{\partial t} = -\sum_{j=1}^{4} r_j \tag{12}$$

The batch was assumed to run under isothermal conditions with constant density and well-stirred. Concentrations for the batch reactor were obtained by calculating the time integrals for different time spans and the starting concentrations for the reaction.

3.1.3 The tubular reactor

The tubular reactor model was set up for each component according to the Dispersion model since the behaviour is similar to that of an ordinary ideal tubular reactor. The model takes into account dispersion, convection and the kinetic reaction mechanism for the feed flowing through the column, see Equation (13).

$$\frac{\partial c_i}{\partial t} = \underbrace{-\frac{v}{\varepsilon}\frac{\partial c_i}{\partial z}}_{Dispersion} + \underbrace{D_{ax}\frac{\partial^2 c_i}{\partial z^2}}_{Convection} - \underbrace{\frac{1-\varepsilon_c}{\varepsilon} r_i}_{Kinetics} \tag{13}$$

The kinetic expression in Equation (13) is partly expressed by void fractions. A more detailed expression of the void fractions can be seen in Equation (14).

$$\varepsilon = \varepsilon_c + (1 - \varepsilon_c)\varepsilon_p \quad (14)$$

The fluid was thought to have constant density was and flowing outside of the packing, setting following void fractions $\epsilon = 1$ and $\epsilon_c = 0$, making ϵ_p insignificant. The process was considered to run under isothermal conditions with convection and dispersion. The axial dispersion coefficient (D_{ax}) was based on calculations of the IEC column to get a realistic dispersion assessment of the tube, see Equation 18 in paragraph **3.2** and was calculated to $2.16 \cdot 10^{-5}$ $m^2 \cdot s^{-1}$. Flow velocity (v) was calculated according to each case study as seen in paragraph **3.4**. The reactions (r_i) were set accordingly to take place by Equations (3-6) presented in paragraph **3.1.1**.

Boundary conditions
To solve Equation (13), initial values and boundary conditions were set at the inlet and outlet of the tube. Initial concentrations for each component *i* were set to zero as the tube was considered to be empty at the start-up, see Equation (15).

$$c_i(t = 0, z) = 0 \quad (15)$$

Dirichlet and von Neumann boundary conditions were set at the inlet and outlet, see Equation (16) and (17) for corresponding boundary condition. Dirichlet was set since the inlet concentration was assumed to be that of the mobile phase while von Neumann was considered no flux of the outlet.

$$c_i(t, z = 0) = c_{in,i} \quad (16)$$

$$c_i(t, z = L) = 0 \quad (17)$$

3.1.4 Simulation approach
All the simulations were carried out in Matlab R2013a. Calculations of the boundary conditions were performed with the script `FVMdiscBV` provided by the Department of Chemical Engineering at Lunds University (24).

Ordinary differential equations
The ordinary differential equations expressed by the reaction models in both the batch and the tubular reactors were solved with `ode15s`. The partial differential equations of concentrations $\left(\frac{\partial c_i}{\partial t}\right)$ were simplified to be ODEs. Further options were used to enhance the accuracy of the ODE solve mechanism by applying tolerance control. Relative tolerance (`RelTol`) and absolute tolerance (`abstol`) were introduced for the computational power with tolerance values set to $10^{-6}$and 10^{-9} respectively.

Partial differential equations
The partial differential equation (PDE) calculations in general were implemented by scripts of the department (24). Only the PDEs describing concentration change in time were assumed to be ODEs. The scripts work numerically by generating matrices of the PDEs with Method of Lines operation by discretisation with the Finite Volume Method (25). For this project, the tubular reactor was meshed by 20 grid points and the first order PDEs were discretised by 2-point backward approximation using `FVMdisc1st`.The second order PDEs were discretised by 3-point central approximation using `FVMdisc2nd`. All discretisations were performed with sparse matrix handling according to script `FVM_JPattern3` retrieved by the department, in order to make the calculations more efficient.

3.2 Chromatography model

IEC was chosen over the SEC to simulate separation of reactor feed. The main reason for this was due to the fact that IEC is the most established purification method and more flexible, but most importantly well suited for continuous processes.

The chromatography process was modelled according to properties expressed by porous packed bed with adsorption. The domain equation is expressed by the Dispersion model, see Equation (13). Void fraction constants used in the simulations are based on experimental values from Tegnér (2015), see Table 3.3.

Table 3.3.Void fraction values retrieved from experimental studies.

Void fraction	Values (-)
ϵ_c	0.321
ϵ_p	0.819

Axial dispersion coefficient was calculated according to Equation (18).

$$D_{ax} = \frac{v \cdot D_p}{Pe} \tag{18}$$

Peclét number (Pe) was assumed a value of 0.5 and the particle diameter (D_p) to $9 \cdot 10^{-5}$ m while the flow velocity expressed in the dispersion term was set to a default value.

Since the chromatography is an IEC, the salt dependency was taken into consideration according to Langmuir adsorption reaction kinetics with salt dependent desorption for the mobile phase, see Equation (19).

$$r_i = k_{kin}\left(H_i c_i\left(1 - \sum_i \frac{q_i}{q_{max,i}}\right) - q_i\right) \tag{19}$$

$$H_i = H_0 * c_s^{-\beta_i} \tag{20}$$

Henry's constant (H_i) is derived from Equation (20), where H_0 is experimentally calibrated Henry's constant, c_s being the salt concentration and β component specific adsorption parameter. The mentioned parameters from Equation (19) and kinetic reaction rates (k_{kin}) were retrieved from the Department of Chemical Engineering at Lund University, see Table 3.4.

Table 3.4. Langmuir adsorption kinetic values shown for each component interacting in the IEC column.

Component	k_{kin} (h^{-1})	H_0 ($mol \cdot L^{-1}$)	β (-)
Lysozyme	293	$1.03 \cdot 10^{-5}$	8.41
Mono	540	$3.05 \cdot 10^{-6}$	8.41
Di	$4.34 \cdot 10^{4}$	$2.63 \cdot 10^{-3}$	4.57
Tri	$4.00 \cdot 10^{6}$	$2.63 \cdot 10^{-5}$	3.00

Maximum concentration of component in stationary phase (q_{max}) was assumed to be 10 $g \cdot L^{-1}$. Component concentration (c_i) and component concentration in stationary phase (q_i) are unknowns' part of the ordinary differential equation. The standard salt concentrations that were simulated for feed, wash and elution are listed in Table 3.5 below.

Table 3.5. Standard salt concentrations used in the simulation.

Salt stream	Concentration ($mol \cdot L^{-1}$)
c_{feed}	0.10
c_{wash}	0.05
$c_{elution}$	0.35

A component mass balance was set up over the stationary phase of the chromatography column in order to define the conditions, see Equation (21):

$$\frac{\partial q_i}{\partial t} = r_i \tag{21}$$

For the mobile phase, Dirichlet boundary conditions were assumed for the equations (22) and initial values were applied as seen in (23).

$$c_i(t,0) = c_{in,i} \tag{22}$$
$$\frac{dc_i(t,L)}{dz} = 0$$

$$c_i(0,z) = 0 \tag{23}$$
$$q_i(0,z) = 0$$

3.3 Desalting

In the chromatography step, a large amount of salt is added to precipitate the adsorbed protein. This concentration of salt needs to be avoided in the reactor, and thus, the salt will need to be separated before the stream is recirculated. This problem is solved by adding a step of membrane separation for the recirculated stream, where the retentate contains a salt concentration similar to that of the feed.

The quantity necessary for the salt dilution is expressed in Equation (24).

$$D_s = \frac{c_{s,in}}{c_{s,out}} \tag{24}$$

Where $c_{s,in}$ was calculated according to the salt concentration coming from the IEC and $c_{s,out}$ was assumed to be the salt concentration of the feed in Table 3.5.

The quantity necessary to concentrate protein is expressed in Equation (25).

$$K_p = \frac{c_{p,out}}{c_{p,in}} \tag{25}$$

Where $c_{p,out}$ was assumed to have same concentration as the original feed in to the reactor and $c_{p,in}$ being the concentration coming from the IEC.

Mass balances are then set up based on volumetric calculations, see Equations (26) and (27).

$$V_{ret} = \frac{V_{feed}}{K_p} \tag{26}$$

$$V_{perm} = \left(D_s - \frac{1}{K_p}\right) \cdot V_{feed} \tag{27}$$

Assuming a constant membrane flux (j) of 50 $L \cdot m^{-2} \cdot h^{-1}$, the domain equation for the filtration system can then be stated by Equation (28).

$$t_{filt} = \frac{V_{perm}}{j \cdot A} \tag{28}$$

3.4 Sensitivity analysis

Neither the IEC column nor the salt filter was calibrated for an efficient handling of the streams. When the entire tubular system was implemented, a sensitivity analysis was performed before any inquiry was made into the reactor processes. The analysis was carried out on the IEC column connected to the salt filter as illustrated in Figure 3.2. The reason for this arrangement was to gain knowledge about the IEC column and the salt filter at the same time since the filter is affected by the IEC column. Constant concentrations were given by the tube reactor. Values for the IEC column were then assumed to be the same for the batch process to make it more realistic.

3.4.1 Analysis arrangement

One factor controlling the separation in the IEC column is the salt gradient (k-value) that is used for both washing and elution. It was therefore chosen to be used in the analysis. This in turn affects the salt filter because of the salt concentration coming from the IEC column. The

simulation was performed by examining the effect of an increased slope of the salt gradient until modelling failure. Before simulating, it was assumed that the chromatography column was able to purify up to 95% of monoPEGs. In the IEC model, it was of interest to see how the yield (see Equation (29)) was affected by the salt gradient. Chromatography yield data was collected by a script (`Simplexpooling`) retrieved from the department (26).

$$Y_{chrom,i} = \frac{\int_{t1}^{t2} c_i dt}{c_{i,load} \cdot t_{load}} \tag{29}$$

In regards to the filter model, it was of interest to see how the area, salt feed volume (V_{sf}) and yield (Y_{chrom}) behaved in relation to each other with varying k-value. Filter time and salt dilution factors K_p and D_s were also investigated out of interest in relation to the salt gradient.

When the analysis was performed, an area was decided for the filter with a reasonable filtration time for a given k-value used in the IEC column.

3.5 Simulation of a batch reactor process

As concluded earlier from the research, the batch reactor is the preferred apparatus for PEGylation in industry. Separation is often handled with IEC columns for separation of the components from the reactor. Yet there is almost no mentioning of recirculation at the moment. For simulation purposes, a regular batch reactor was set up and connected to an IEC column with no recirculation as depicted in Figure 3.1.

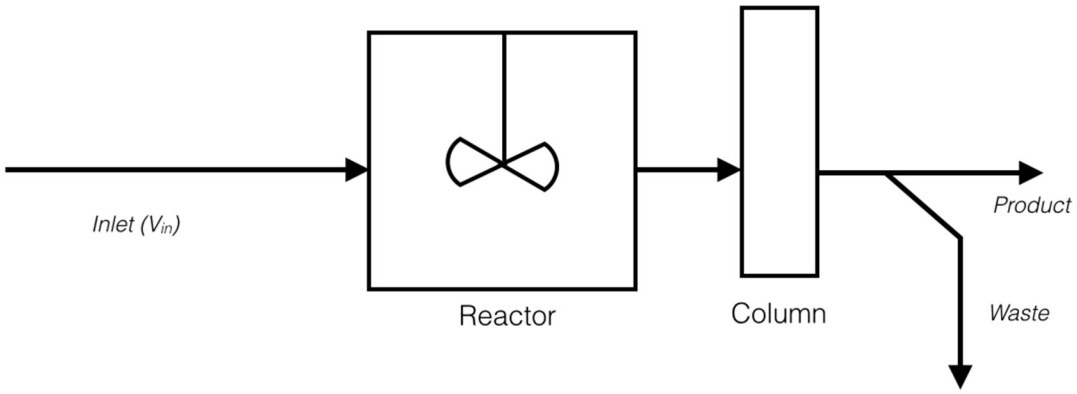

Figure 3.1. Schematics over the batch process in connection to an IEC column. Outflow from the IEC column is divided into pool streams of waste and product.

The batch reactor process was modelled in accordance to the models presented under paragraphs **3.1** and **3.2**.

3.5.1 Validation

As already stated under paragraph **3.1**, batch experimental data was applied in this modelled set up. Before any analyses were made, the batch reactor first had to be validated in accordance to experimental data. This was performed by using provided k-values for the reaction model and setting up initial concentrations according to the experimental procedure, see Table 3.1.

3.5.2 Reaction termination point

After validating the model, an appropriate time for the termination of the reaction had to be found. In this simulation it was assumed that the industrial termination point for the PEGylation process is when highest yield of monoPEGylated proteins. To find the yield it was assumed that the reaction occurred under excess of both $NaBH_3CN$ and PEG since biopharmaceutical proteins are costly in relation to the reactants. The yield was defined, where component *i* in this case is monoPEGylated proteins and $c_{Lys,in}$ is the initial concentration of lysozyme, see Equation 30.

$$Y_{reac,i} = \frac{c_{i,out}}{c_{Lys,in}} \tag{30}$$

Using the in-built Matlab function `fmincon`, an objective function was defined to find the desired maximum yield of monoPEGs, see Equation (31).

$$objective = -Y_{reac,mono} \tag{31}$$

Decision variables were then determined for the objective in two different cases, see **Case I** and **II** below.

Case I – Reactant constraints

The relationship of initial concentration of PEG and $NaBH_3CN$ to lysozyme was investigated, see Equations (32,33) below. These equations were used as decision variables (dv_1 *and* dv_2) seen in Equations (34,35).

$$x_{PEG} = \frac{c_{init,PEG}}{c_{init,Lys}}, x_{CBH} = \frac{c_{init,CBH}}{c_{init,Lys}} \tag{32,33}$$

$$dv_1 = x_{PEG}, dv_2 = x_{CBH} \tag{34,35}$$

The objective was then computed with a time span of three hours reaction time to be the same as in the batch experiment.

Case II – Reactant and time constraints

Like in previous case, an investigation was made with decision variables dv_1 and dv_2. Information gained from dv_1 and dv_2 in previous case were used and applied to the same objective function as guessing points. The difference in this case compared to the first case was the addition of time as a third decision variable (dv_3), expressed in Equation (36).

$$dv_3 = \int_0^t dt \tag{36}$$

Optimisation set-up

The objective functions were simulated with the built in "interior-point" algorithm. In terms of enhancing accuracy, the `fmincon` was regulated through tolerance of the objective function (`TolFun`), decision variable tolerance (`TolX`) and the finite difference estimation of the objective function (`FinDiffRelStep`). Same settings were also adapted for the IEC. Applied function tolerances can be found in Table 3.6.

Table 3.6. Values of parameters used by `fmincon` to achieve improved optimisation.

Constraint	Tolerance
`TolFun`	10^{-12}
`TolX`	10^{-12}
`FinDiffRelStep`	10^{-3}

3.5.3 System performance calculations

After the sensitivity analysis was performed and the yields were found for each case, a system performance evaluation was performed. Productivity and yields were determined for the reactor simulation process as defined in Equations (29,30,37,38).

$$\mathrm{Pr} = \frac{c_{prod,mono} \cdot V_{prod,mono}}{(t_{reac} + t_{chrom})} \tag{37}$$

$$Y_{sys,i}^{ss} = Y_{reac,i} \cdot Y_{chrom,i} \tag{38}$$

Where component *i* for all yield equations was calculated for both mono- and multi-PEGylated proteins. For chromatography yield ($Y_{chrom,i}$), t_2 and t_1 are cutting points for the pooling concentrations for component *i* and t_{load} as the loading time.

Productivity (Pr) defined by $c_{prod,mono}$ and $V_{prod,mono}$ being concentration and volume for monoPEGs respectively in the "Product" pooling stream in Figure 3.1. Reactor time (t_{reac}) for the batch reactor was calculated as the reaction time plus dead time (assumed to 0.5 hours). Reactor time was then added with the separation time of the chromatography (t_{chrom}).

The system yield ($Y_{sys,i}^{ss}$) was based on reactor steady-state condition for component *i*. It was calculated for both mono- and multiPEGylated proteins coming out of the reactor ($Y_{reac,i}$) multiplied to the IEC column yield ($Y_{chrom,i}$).

3.6 Simulation of a tubular reactor process

After simulating the batch process in Matlab, efforts were made to achieve adequate results using a recirculated process with a tubular reactor. The tubular reactor simulation was modelled in accordance to the models presented under paragraphs **3.1-3.3**.

Unlike the batch model, the tubular reactor does not hold the reactant but rather lets the PEGylation occur in pulses through the reactor. After passing through the IEC column (which is identical to the previous model), the stream is divided into three cuts where the one containing an abundance of native protein is recirculated. A sketch of the process is displayed in figure Figure 3.2.

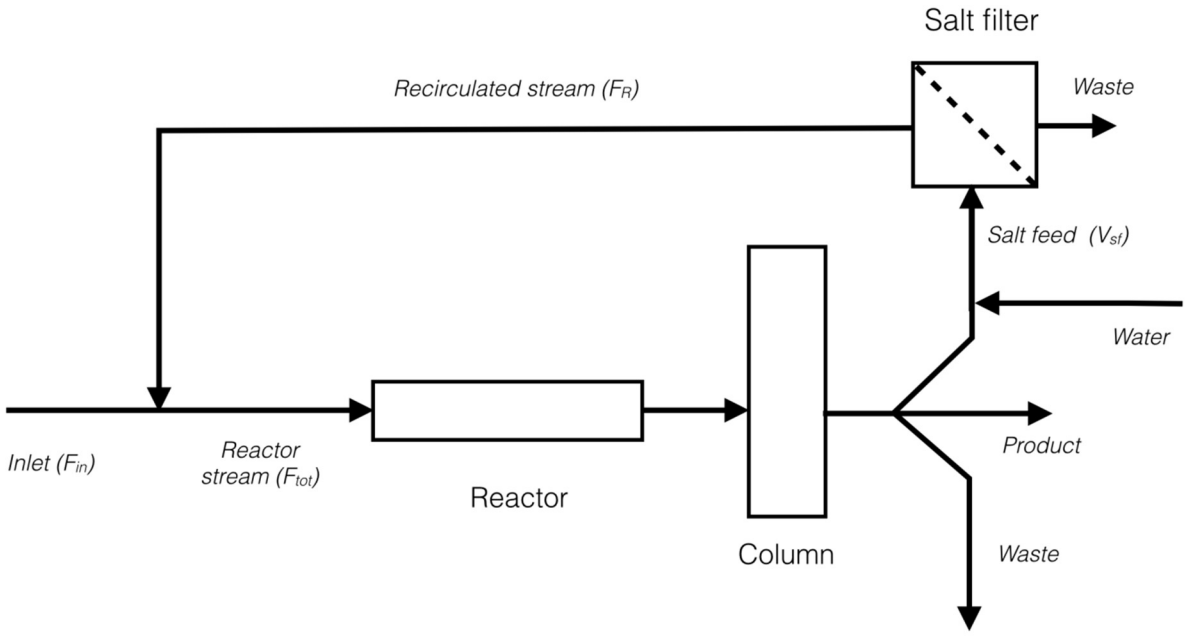

Figure 3.2. Schematics over the tubular reactor attached to an IEC column. Outflow from the IEC column is divided into pool streams of waste, product and a feed to the salter filter used for recirculation.

In order to avoid too low levels of affinity of the reactor components in the chromatography steps of the recirculation streams, the purified stream was diluted before recirculation. The protein in the diluted stream was then reconcentrated using a salt filter and was then fed to the tubular reactor. In this simulation it was assumed that the recirculation practice was performed by having a constant flow in to the reactor. Consequently, as illustrated in Figure 3.2, this means that the inlet flow (F_{in}) will decrease so that it can merge with the recirculated stream (F_R) and still retain the same flow capacity in the reactor stream (F_{tot}).

3.6.1 Tubular process analysis

To simulate similar conditions to the batch reactor, it was thought that the process also reacted in excess of PEG and $NaBH_3CN$. Three cases were set to investigate different reaction termination points. Recirculation was considered for each case.

Case I – By-product constraint
The reaction was terminated at a yield where enough amount of formed by-product was considered to be tolerable while keeping as high yield of monoPEGs as possible. A PEGylation reaction curve was generated and a reasonable termination point (residence time) of the reaction was set.

Case II – Residence time
Since the tube length and the residence time are proportional to each other (see Equation 39), a decrease in tube length will have the same effect on the residence time.

$$\theta = \frac{z}{v} \tag{39}$$

Where the residence time (θ) is expressed in hours, z being the tube length in meters and flow velocity of the tubular reactor (υ) in $m \cdot s^{-1}$. For this purpose an evaluation was made with `fmincon`. The objective function was defined by Equation (40) and the residence time was then used as a decision variable (dv_4).

$$dv_4 = \frac{x}{v} \tag{40}$$

The optimisation was arranged in the same manner as mentioned in **Optimisation set-up**, paragraph **3.5.2**.

Case III – Pareto front
A parameter sweep was set up over the tubular reactor to extract data about the productivity and the yield. The sweep was performed by altering the tubular flow velocity, i.e. the residence time, while keeping the same tube length from the validation procedure. After obtaining the Pareto front, an optimal Pareto point was chosen by visual estimation. From this Pareto point, a velocity could be extracted and then used for the system simulation.

Like noticed, both **Case II** and **III** investigates residence times. The main difference between the cases is that **Case III** is not affected by any coded objectives and could give different results.

3.6.2 System performance calculations
Productivity and yields for all three cases implemented in the tubular reactor schematics were calculated according to Equations (29,30,37,38).

4 Results and discussion

4.1 Sensitivity analysis

Like mentioned, a sensitivity analysis was first carried out over the IEC column and a salt filter in a series. The salt gradient (k-value) was steadily increased until failure was met. Four IEC chromatograms were registered, see Figure 4.1.

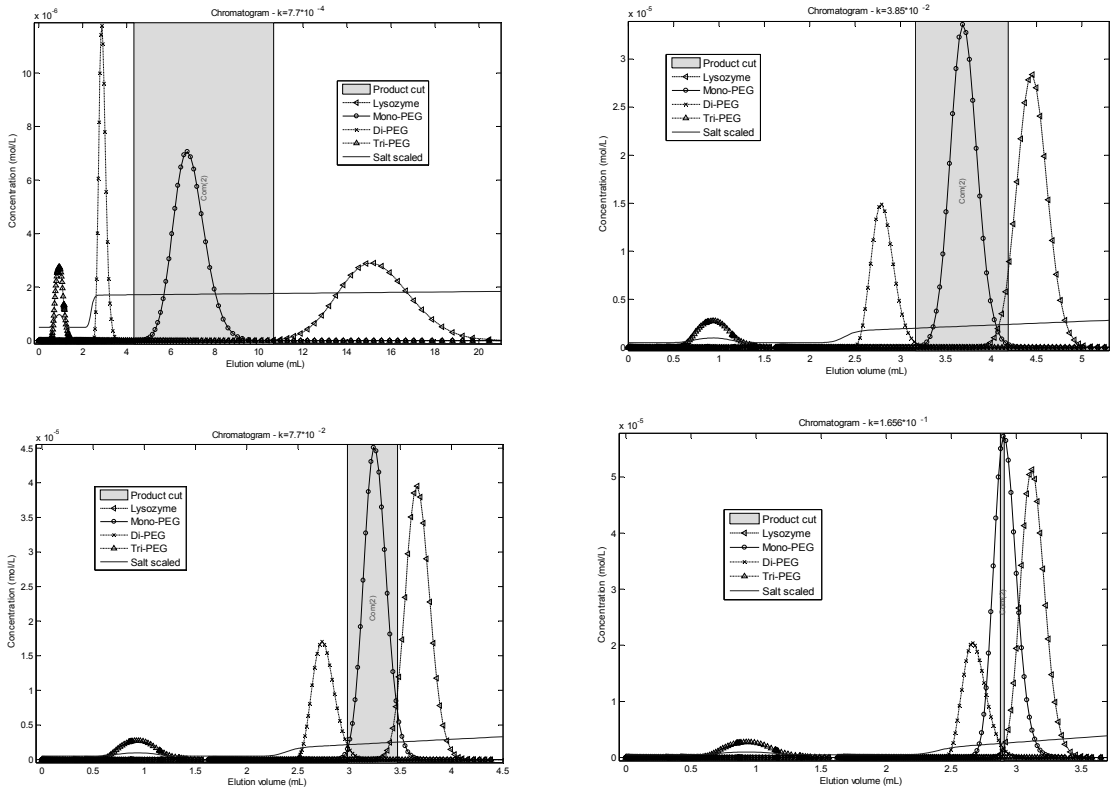

Figure 4.1. Four chromatograms showing the separation evolution of an IEC column when increasing the k-value read from A-D.

First noticeable changes in the separation are the cuts, as they become narrower with higher k-values. The main reason for this phenomenon is because of the purity requirements that have to be met. As the salt gradient increases, the elution occurs faster thereby peaks eluting at smaller elution volumes. A consequence of this is that components in the IEC column get closer to each other and mix together after a certain point. As they mix together, the cuts become smaller until the components are too mixed and the separation will fail. Chromatogram D represents the most extreme case, borderline to failure.

This information shows that there are more factors to take into consideration when choosing a reasonable k-value for separation. One cannot only consider purity of the product and faster elution time but also the yield of how much of the product it is possible to recover from the column. The column yield was then considered to be plotted against the k-value. Because the salt filter area was desired to be calculated it was also included along with the salt feed volume (V_{sf} in Figure 3.2) to see how the outgoing stream from the filter was affected, see Figure 4.2.

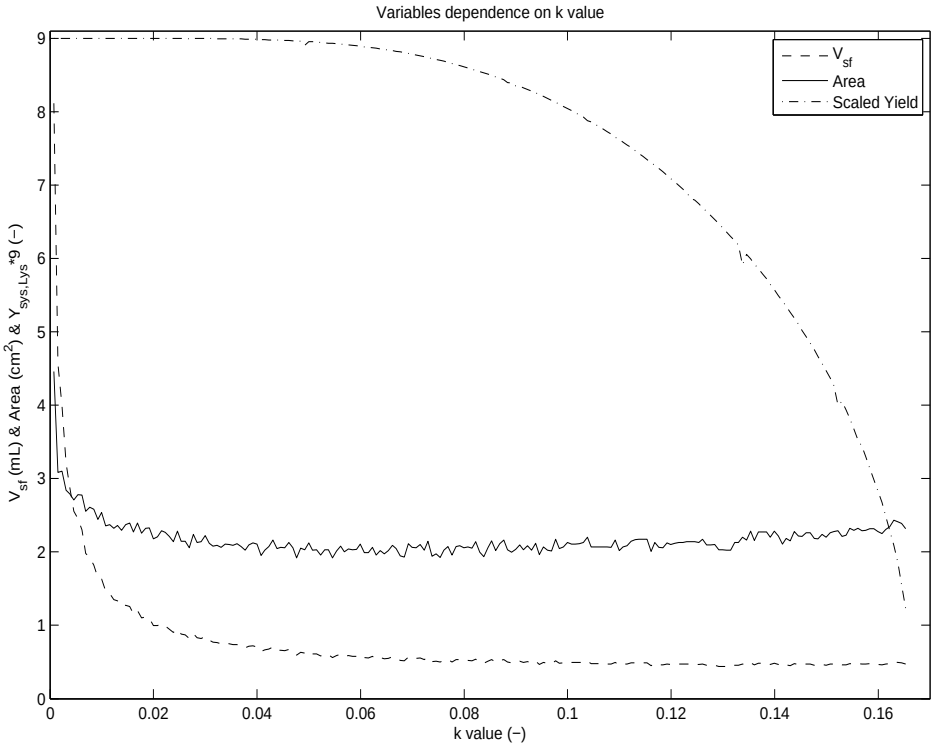

Figure 4.2. Illustration of recirculation volume and area from the salt filter with scaled yield(9=100%) dependent on the k-value.

By studying Figure 4.2, it is worth noting that the filter area seems to increase after a certain point. As known, it is the relationship between permeate volume and filtration time that is the cause of this phenomenon. The filter time is determined by the elution volume cuts, which as described by the chromatograms above decreases steadily with higher k-value. For that reason it must be the permeate volume that affects the area increase. A higher k-value provides a higher protein concentration since the peaks become narrower and of course a higher salt concentration. After a certain point the protein concentration factor (K_p) reaches somewhat of a steady-state while naturally the dilution factor (D_s) continues to increase as the salt gradient increases as can be seen in Figure 4.3 below. By viewing the salt volume feed in Figure 4.2 in relation to D_s and K_p in Figure 4.3, shows that it goes to steady-state while the salt concentration increases while the protein concentration is at almost same level. This means that the dilution of salt feed in relation to concentrating the protein becomes a more dominant factor which affects the permeate volume. This in turn affects the filter area which should be payed attention to and handled wisely when choosing a k-value.

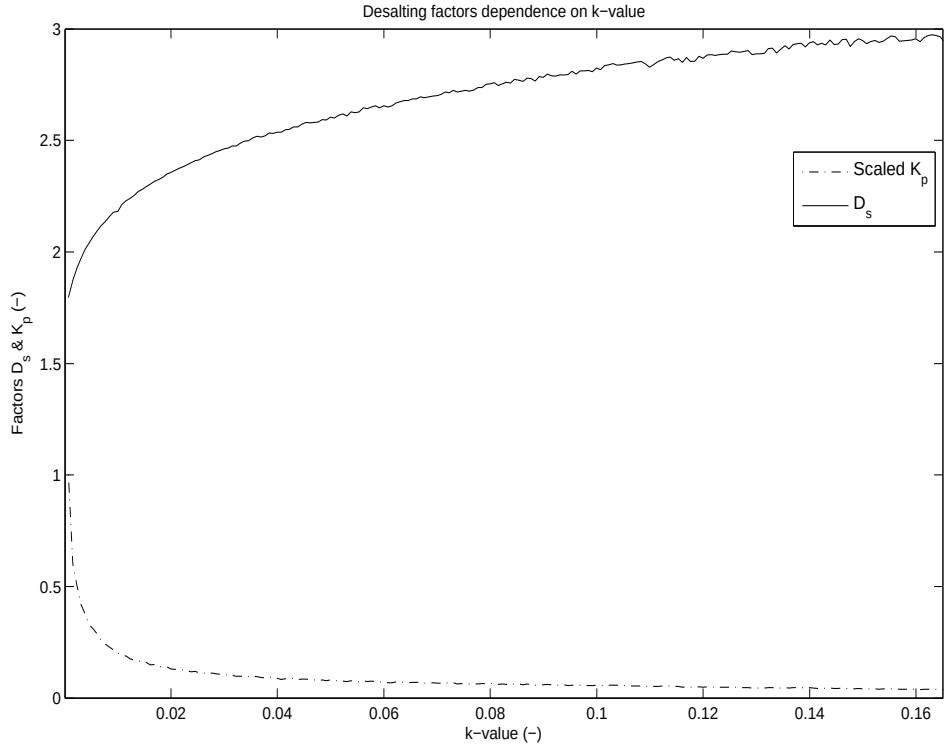

Figure 4.3. Dilution factor (D_s) and protein concentration factor (K_p) for the salt filter plotted against the k-value.

Like shown in Figure 4.2, a fairly high k-value can be placed in order to increase the productivity while still retain an effective filter area and yield. To keep a fairly high recover while still running the IEC column efficiently and also having in mind the filtration time, a column yield of 95% was chosen. The filtration time averaged about 10 minutes which was considered to be efficient. Obviously, 95% is a bit of a reach but aiming higher is better to compensate for spillage. Corresponding k-value to the 95% column yield was retrieved from the calculation and was revealed to be 0.0838. Considering that the plotted graph of the area displays unstable behaviour, a mean value was calculated. A mean was calculated from a region where k-values differed ±10% from the chosen k-value. The calculations returned an average filter area of about 2.06 cm^2. One filter is required in this setup considering that the filtration time is less than the reactor residence time. However, further optimisation research of the process could increase its productivity. For example the flow could be increased to the tube reactor and then combining it with an SMB setup. An increase in productivity would in essence also mean an increase in filter area to handle larger volumes.

Even though the productivity of the IEC column is considered to be maxed in this simulation, it could affect the whole setup. It is obvious that not every possible angle of realistic features is simulated. For example, it should be noted that this simulation does not take fouling into consideration for neither the salt filter nor the IEC column. Such high k-value could render an increase in pressure drop and decrease in productivity over time. However, one should not be shy about pressing the performance to a certain degree. Sufficient washing of the columns according to manufacture specifications usually keeps the columns unimpaired. Also, the productivity gained by using ion-exchange columns compared to other forms of separation methods in the pharmaceutical industry is usually sufficient enough to cover unforeseen ex-

penditures. In this project, fouling would have been most interesting for the salt filter since the same conditions would be applied for IEC columns in both schematic cases. In a broader sense it would have been interesting to see how much the fouling affects productivity.

In general, high k-values in regards to time elution efficiency (i.e. productivity) should also be weighed in relation to buffer costs that are often expensive. As noticed in chromatograms above, there is a certain point where k-values stops being relevant for efficiency and only brings about unnecessary costs for small gains in efficiency. This is further supported by studying the filter time (Figure 4.4) which goes to a steady state after a while.

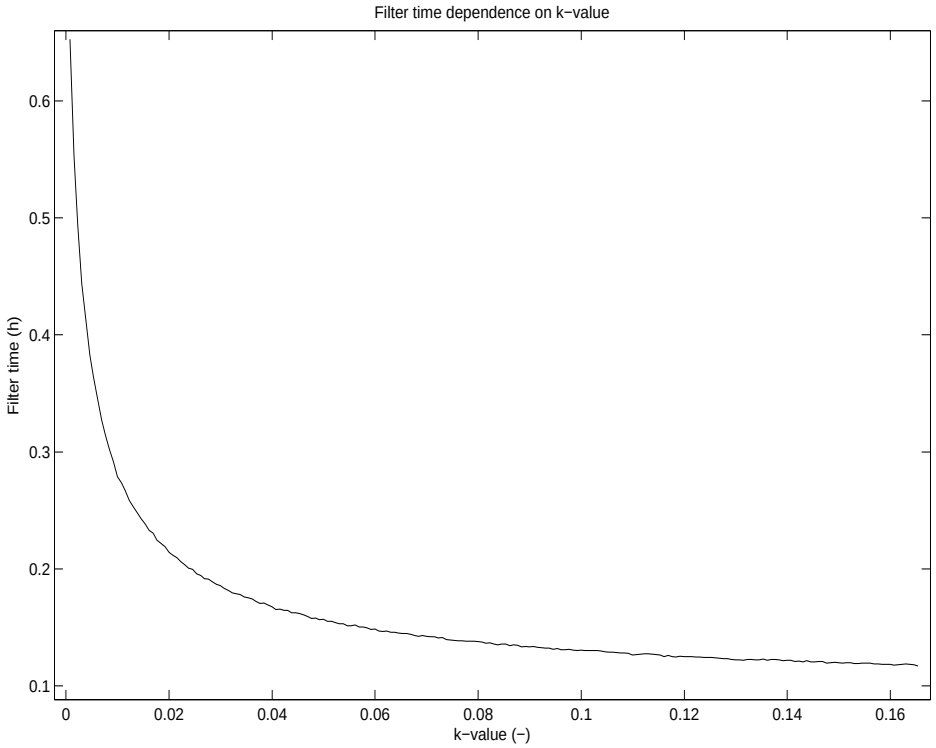

Figure 4.4. Filter time dependency on salt gradient (k-value).

4.2 The batch process

4.2.1 Validation

First the batch model had to be validated against the experimental data. The results showed an adequate fit with only two outliers for the last lysozyme and monoPEG data points, see Figure 4.5.

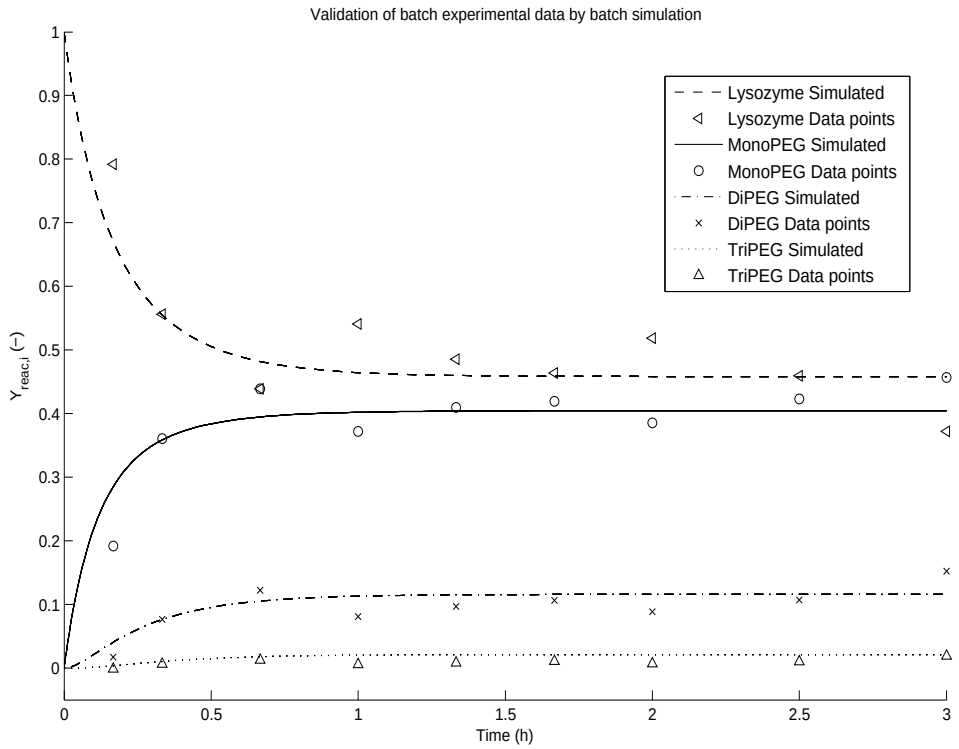

Figure 4.5. Validation curve of experimental batch simulated in Matlab. The points in the graph represent experimental measure points while the lines are simulated values.

The reaction time is in total three hours, but slows down within an hour. A reason for the slow down effect can be explained by lack of PEG and/or CBH in the reaction. The experiment managed to generate about 40% monoPEG and approximately 10% multiPEG based on the initial concentration of lysozyme.

4.2.2 Optimisation

Following the validation, an optimal termination point was then tried to be found for the reaction process with `fmincon`. As specified earlier, two cases were investigated for the batch reactor. The main results of the `fmincon` examination can be seen in Table 4.1.

Table 4.1. Ratio factors for results of fmincon. I: investigation of the relationship between $NaBH_3CN$ and PEG. II: optimisation with $NaBH_3CN$ and PEG in excess with time as decision variable.

Case	x_{CBH} (-)	x_{PEG} (-)	Residence time (h)
I	16.51	16.51	3
II	16.71	16.71	2.872

Case I – Reactant constraint

The problem was solved by the created objective function of determining the highest reactor yield ($Y_{reac,mono}$). By using `fmincon`, residence time was locked to 3 hours, to be same as the experimental data and the ratios x_{PEG} and x_{CBH} were fined tuned. Factors for each ratio were found to be 16.51. A contour plot was created to get a better understanding of the relationship between the ratios of PEG and CBH along with found yield optima, see Figure 4.6.

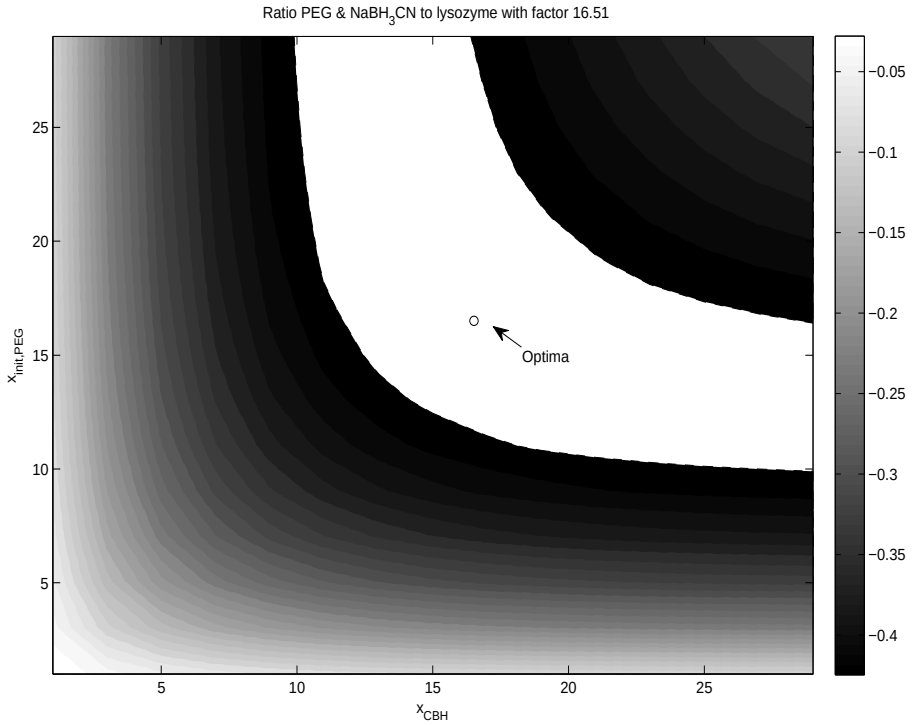

Figure 4.6. Contour plot of ratio x_{PEG} vs x_{CBH} with objective yield optima at ratio 16.51 for both factors.

As can be seen the problem is of convex nature and the solved objective can therefore be seen as satisfied. Interestingly the plot also shows how wide the area is for acceptable solutions. One could, according to the contour plot above be able to achieve the satisfactory results but for different ratios of PEG and CBH. For instance, depending on the case of PEGylation, the

PEG could be more expensive in relation to CBH regarding this type of reaction. Theoretically it would be possible to lower the x_{PEG} and increase or stay at the same x_{CBH} as indicated by the contrast of the convex area in the contour plot. However, it should not be taken lightly, because it is dependent on tolerances and algorithms used in Matlab for the `fmincon`. The area of satisfactory solutions could very well be much narrower than what is illustrated in the contour plot.

Case II – Reactant and time constraint

The second optimisation was performed with previous factors as guessing points but in addation having time as a decision variable, see Figure 4.7. Optimal time of termination for the reaction was determined to be 2.872 hours with an x_{CBH} of 16.71 according to computation from `fmincon`.

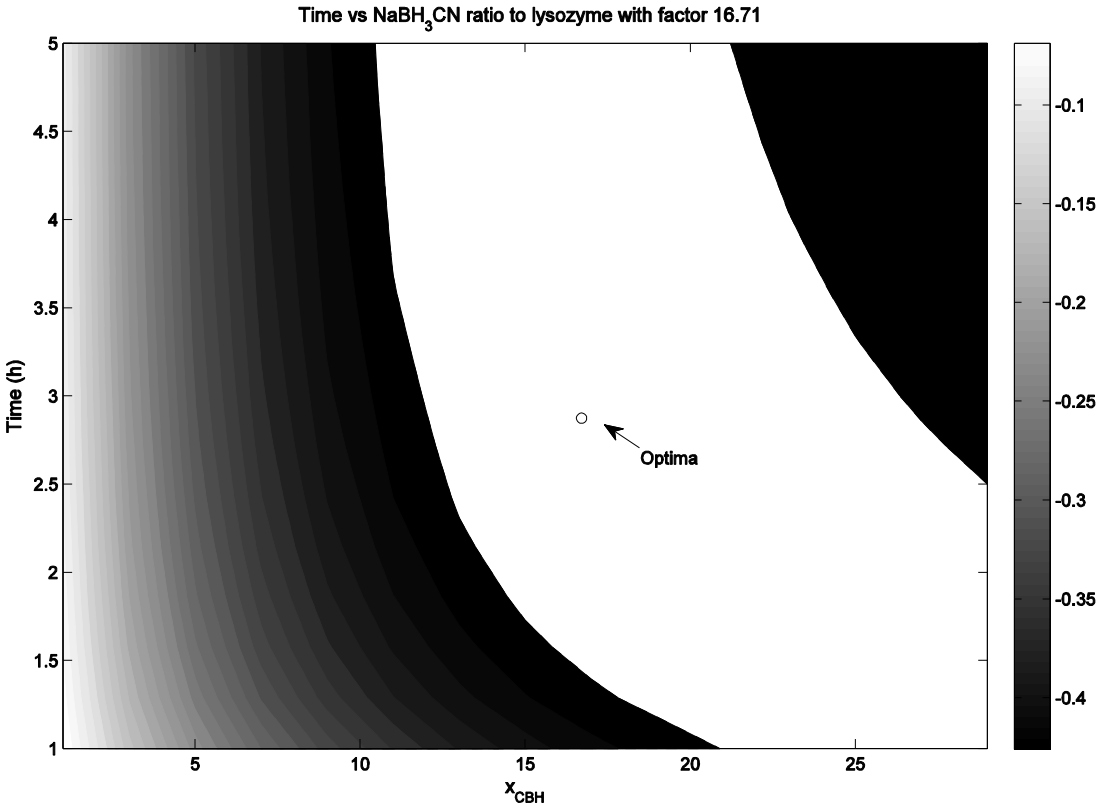

Figure 4.7. Contour plot of time vs x_{CBH} while PEG-ratio is locked with objective yield optima at time of 2.872 hours and x_{CBH} ratio 16.71.

Like the previous contour plot, the figure above also displays same type of convex behaviour and even larger area of satisfactory solutions. It too could be regarded as satisfied. And like stated in previous discussion, the large area of satisfactory solutions in this contour plot could be deceptive and should not be taken lightly.

4.2.3 System performance analysis

By comparison (see Table 4.2 below), **Case II** performs better in almost all aspects. Even though the the initial concentraiton ratio for PEG and CBH is increased by 1%. This seems negligable compared to the fact that 5% of the reaction time is cut off. Conversely, it also means the batch yield remains the same even though the process is cut short. Even the productivity is increases as one would expect since the batch time decreases. Though waste

yield is still rather high in both processes and comparatively similar. Because of the stated differences, **Case** II was chosen to represent the batch schematics.

Table 4.2. Various yields and productivity for the entire process presented. The highlighted row shows that case which was chosen to represent the batch schematics.

Case	$\mathbf{t_{res}}$ (h)	$\mathbf{Y_{reac,mono}}$ (-)	$\mathbf{Y_{chrom,mono}}$ (-)	$\mathbf{Y_{sys,mono}}$ (-)	$\mathbf{Y_{sys,waste}}$ (-)	**Pr** ($g \cdot h^{-1}$)
I	3.000	0.4378	0.9871	0.4322	0.2535	0.0123
II	2.872	0.4378	0.9892	0.4331	0.2514	0.0126

The batch reactor was then simulated after the acquired values from **Case II** in Table 4.1, see Figure 4.8.

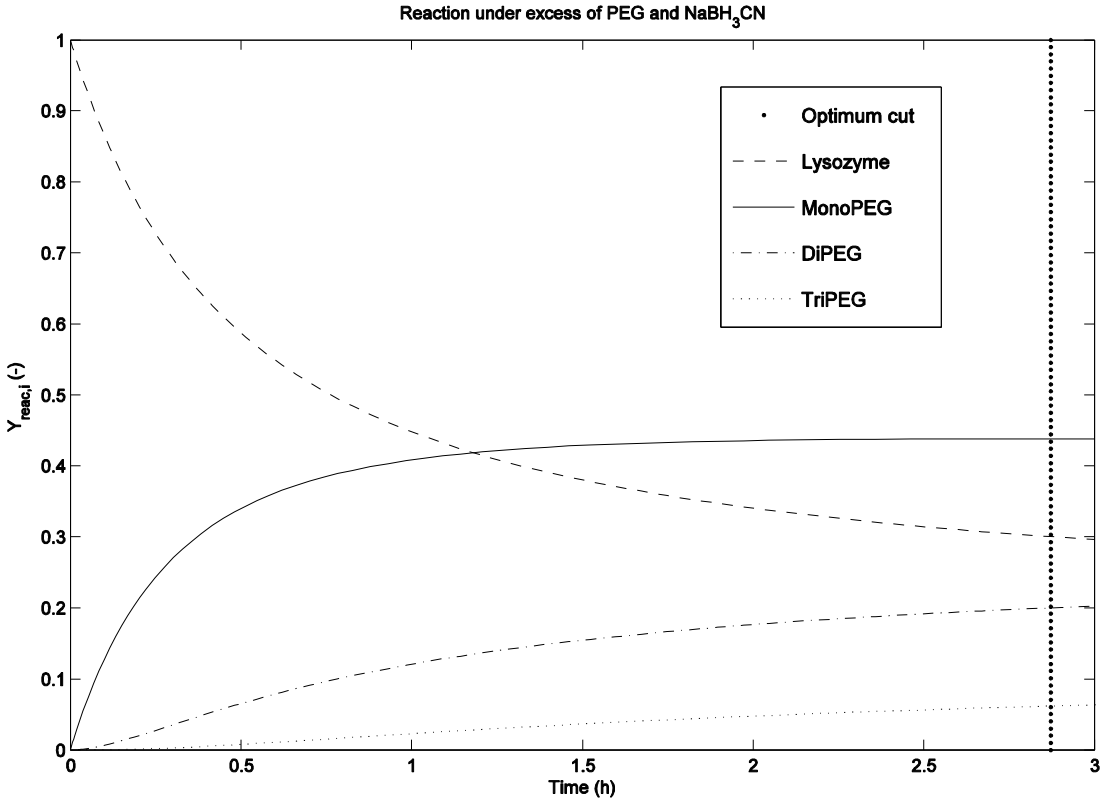

Figure 4.8. Representation of the batch reactor simulated in excess of $NaBH_3CN$ and PEG with the optimal reaction cut displayed in the graph.

As shown in the graph, the cutting point could be made even earlier to increase both productivity and product yield while reducing waste yield. However, this result is due to the chosen objective function for the case. More objectives could have been added to improve the optimisation. An example would be to optimise the product yield in relation to waste yield to minimise the waste and still keep high monoPEG production.

4.3 The tubular process

First the tubular model had to be validated against the batch experimental data, see Figure 4.9.

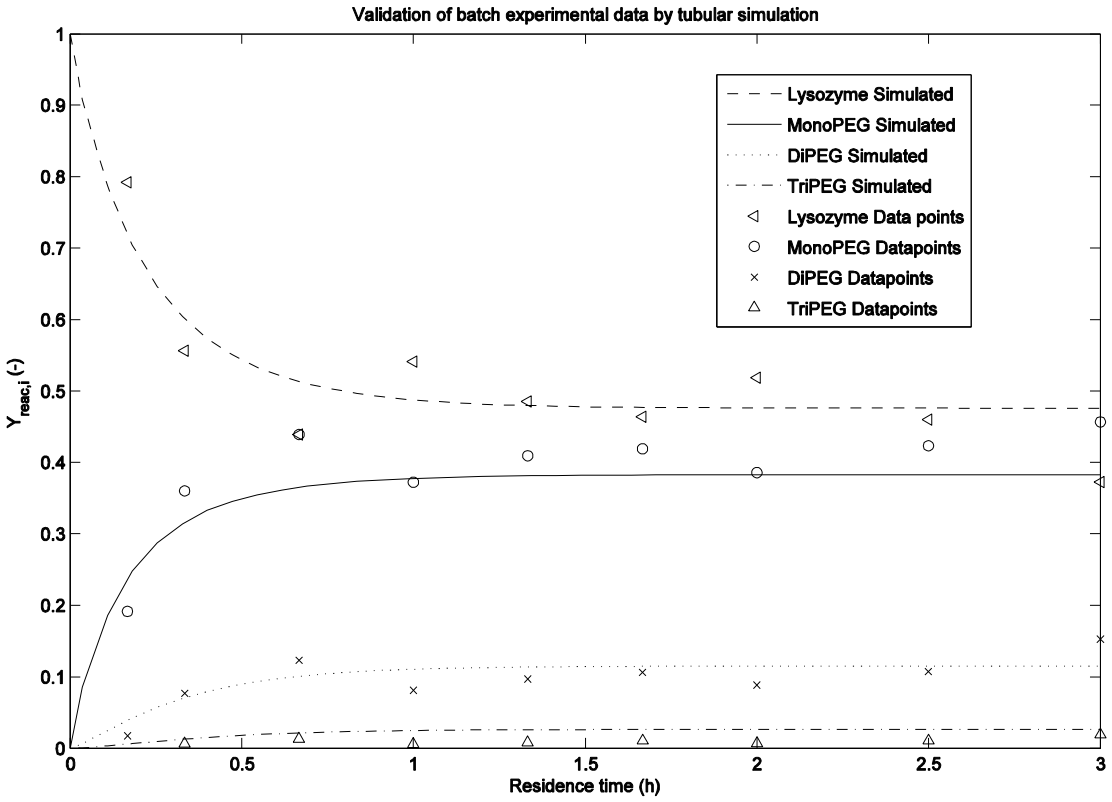

Figure 4.9. Validation of the tubular reactor model against batch experimental data.

The resulting graph showed in general an adequate fit with only the simulated monoPEGylation coming a bit short of fitting the data points. Though, this is not of a concern since the profile merely depends on fine tuning of the system. Like number of grid points, column residence time; i.e. column length and velocity which in turn affect other computational operations. It should also be noted that the x-axle is displays the residence time and can be translated to column length. What is thus shown in the plot is the concentration profile of the reactor. This is later used to determine tubular specifications.

4.3.1 Case I – By-product constraint

For the first case the termination was decided on a point which seemed to be reasonable. The reaction graph presented by the batch reactor (Figure 4.8) was studied in order to determine a termination point since the reaction probably would be similar. A point was decided when the yield of DiPEG ($Y_{reac,di}$) was below 10% to minimise formation of by-products. The point was cut for each recirculation cycle like seen in Figure 4.10 and productivity and yields were calculated for the specific process at steady-state.

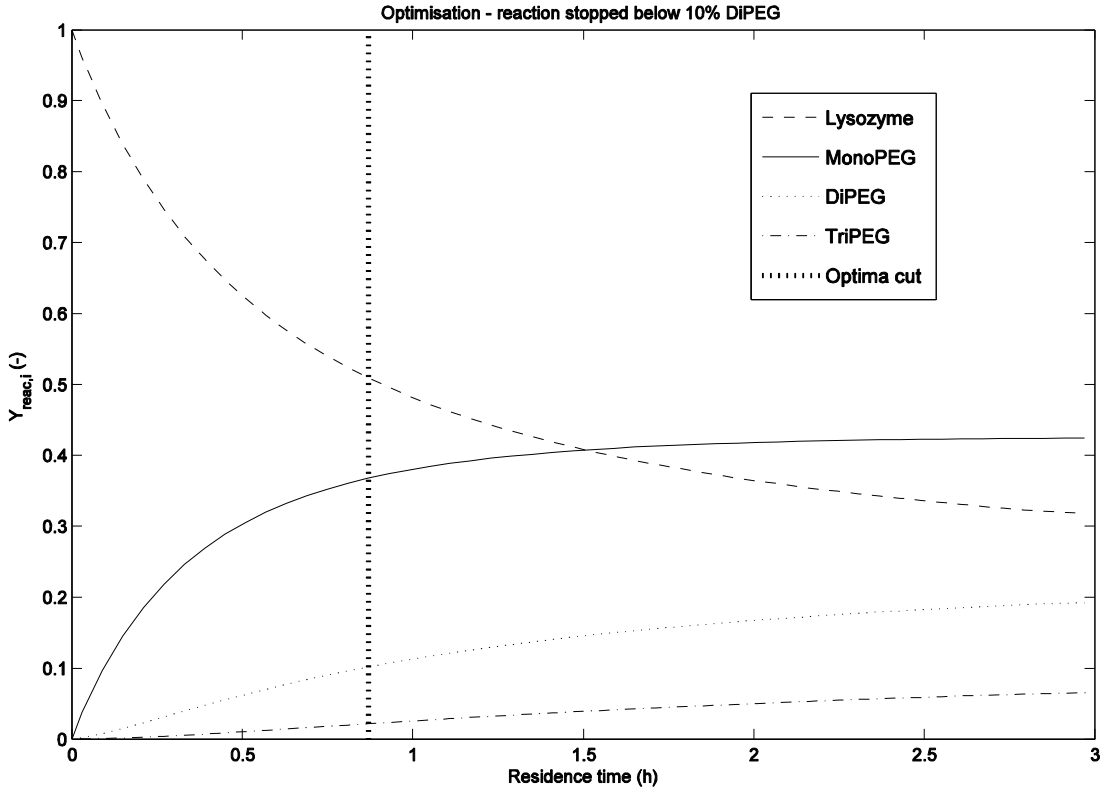

Figure 4.10. Illustration of termination point for the 0th recirculation cycle. DiPEG yield from the reactor is below 10% with residence time of 0.81 hours (Product cut).

Running the process with the specified termination point presented at the last cycle a relatively high productivity of 0.0217 $g \cdot h^{-1}$. It is mainly due to lower residence times, like presented for the 0th cycle which was 0.81 hours. From the graph it is visible that even though the reaction is cut short, a relatively high monoPEG yield is obtained from the reactor. For this case, it was generated that eight salt filters were needed in order to keep up with the stream demand.

Steady-state (SS) for the recirculation was reached after approximately five cycles, as can be seen in Figure 4.11 below. The other cases show similar effect of converging after five cycles.

A complete compilation of the obtained data can be viewed in the **System performance analysis** (paragraph **4.3.4**).

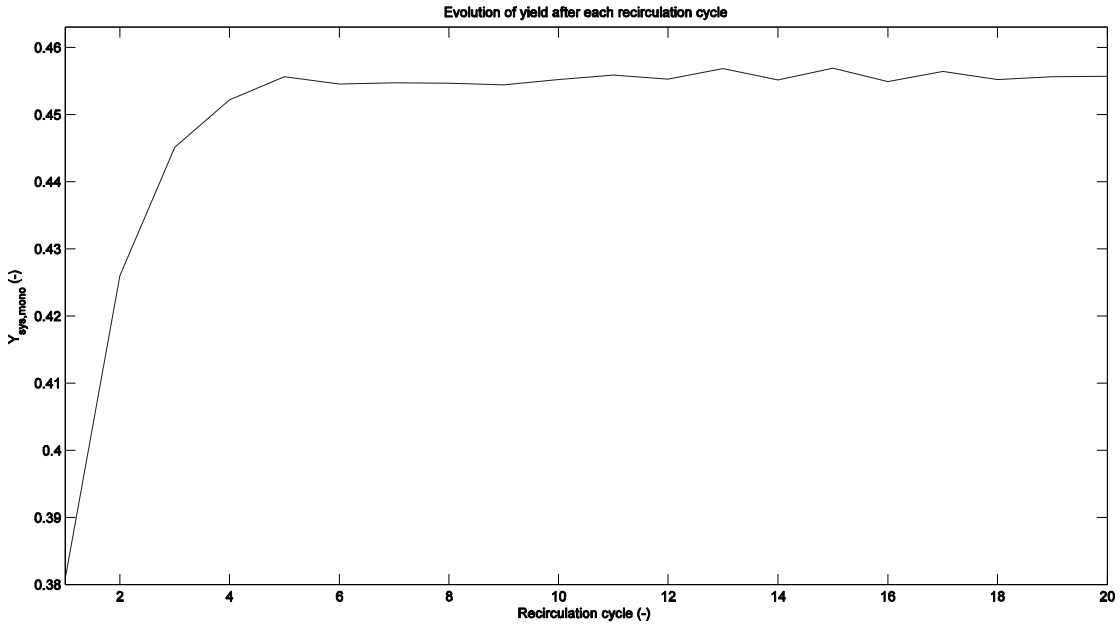

Figure 4.11. Illustrating system monoPEG yield after each recirculation cycle. Note: here the cycle starts at 1, which is referred in this work as being the 0^{th} cycle.

The figure shows a shaky SS which could probably be derived from the tolerances converging differently after each cycle. It is interesting to see that it takes the same amount of cycles to reach steady-state for the three cases. The reason for this could lie in how the recirculation stream is introduced with the inlet feed (F_{in}) to the reactor as shown in Figure 3.2. In this project, a subtraction is made of the inlet feed with the recirculation stream (F_R) to keep the reactor feed constant which could be the reason behind the SS. Perhaps the yield could reach even higher values.

4.3.2 Case II – Residence time

The second case which was simulated with fmincon displayed a long reaction time compared to the experimental one. However, one should not forget that this simulation is assumed to be in somewhat different conditions (excess of PEG and CBH). The graph of the reaction can be viewed in below.

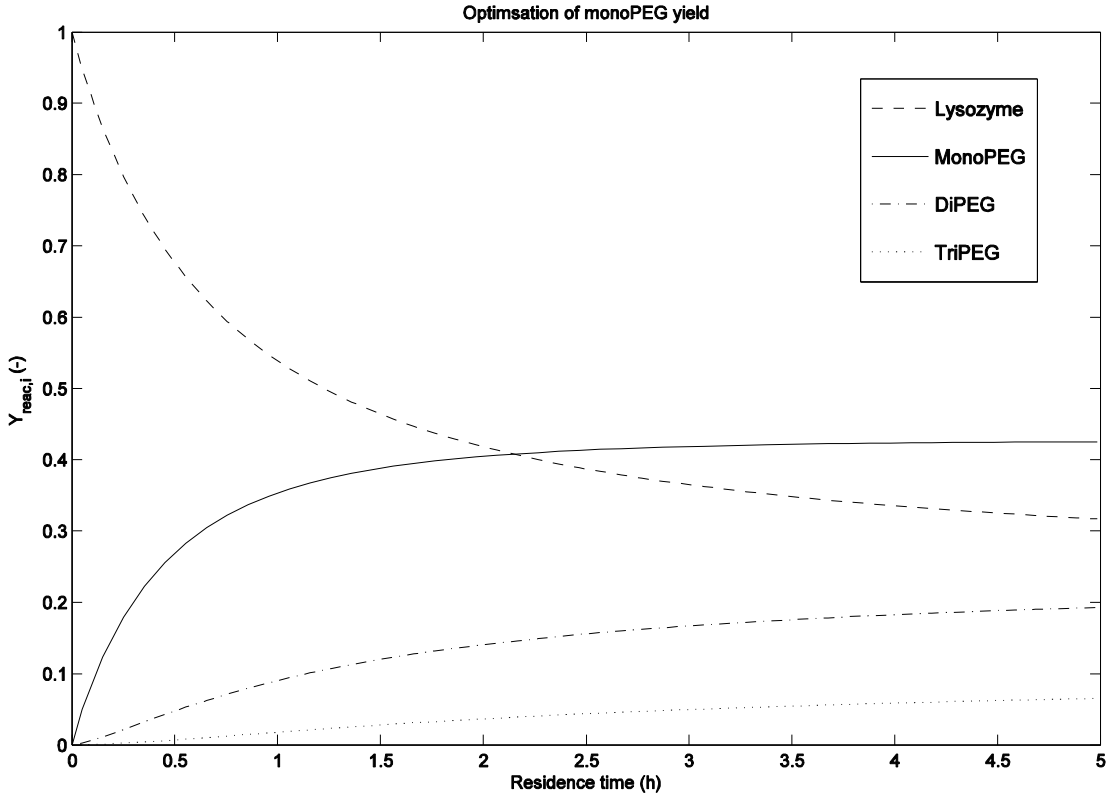

Figure 4.12. Illustrating termination point at five hours by simulating with fmincon under time constraint.

When the entire process was run according to the termination point, a relatively low productivity of 0.65 $g \cdot L^{-1} \cdot h^{-1}$ was reached with a residence time of five hours, an increase of 67% of full reaction time. Like previous cases, steady-state was reached after the five cycles. For this case, it was generated that six salt filters were needed in order to keep up with the stream demand.

A complete compilation of the obtained data can be viewed in the **Case summary** (paragraph **4.3.4**).

4.3.3 Case III – Pareto front

Third case studied the tubular reactor process by having the flow velocity as the decision variable. From this it was able to create a Pareto front of productivity versus yield of monoPEGylated lysozyme, see Figure 4.13.

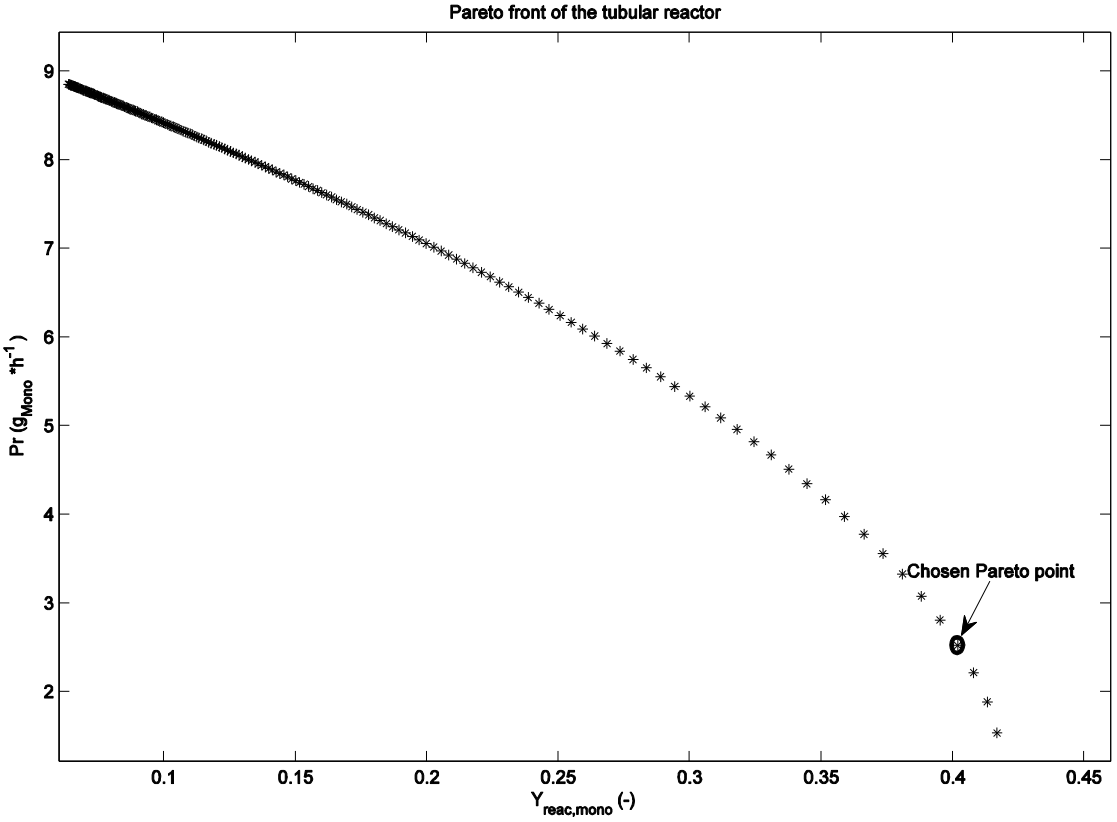

Figure 4.13. Illustration of Pareto front for the tubular reactor with flow velocity as decision variable. Productivity (Pr) plotted against monoPEG yield ($Y_{reac,mono}$) for the tubular reactor.

Choosing Pareto point is not an easy task since it depends on the process. Like obvious, it is a loss of either or when moving along the graph. For this project it is wise to stay on the right side of the curve, i.e. high yield. The reason for this follows the same purpose as brought up for the batch reactor. Biopharmaceuticals are studied in this project and they are costly. Nevertheless, one should always try to squeeze out some extra productivity if it is possible. In this study a yield of 0.40 monoPEGylated lysozyme was chosen as not to differ all too much from **Case II** and still gain a lot of productivity. For this case, it was generated that seven salt filters were needed in order to keep up with the stream demand.

The productivity was read from the Pareto front figure and returned 2.5 $g \cdot L^{-1} \cdot h^{-1}$. Same productivity value could then be translated to a velocity, since it was the decision variable, which can be seen in Figure 4.14.

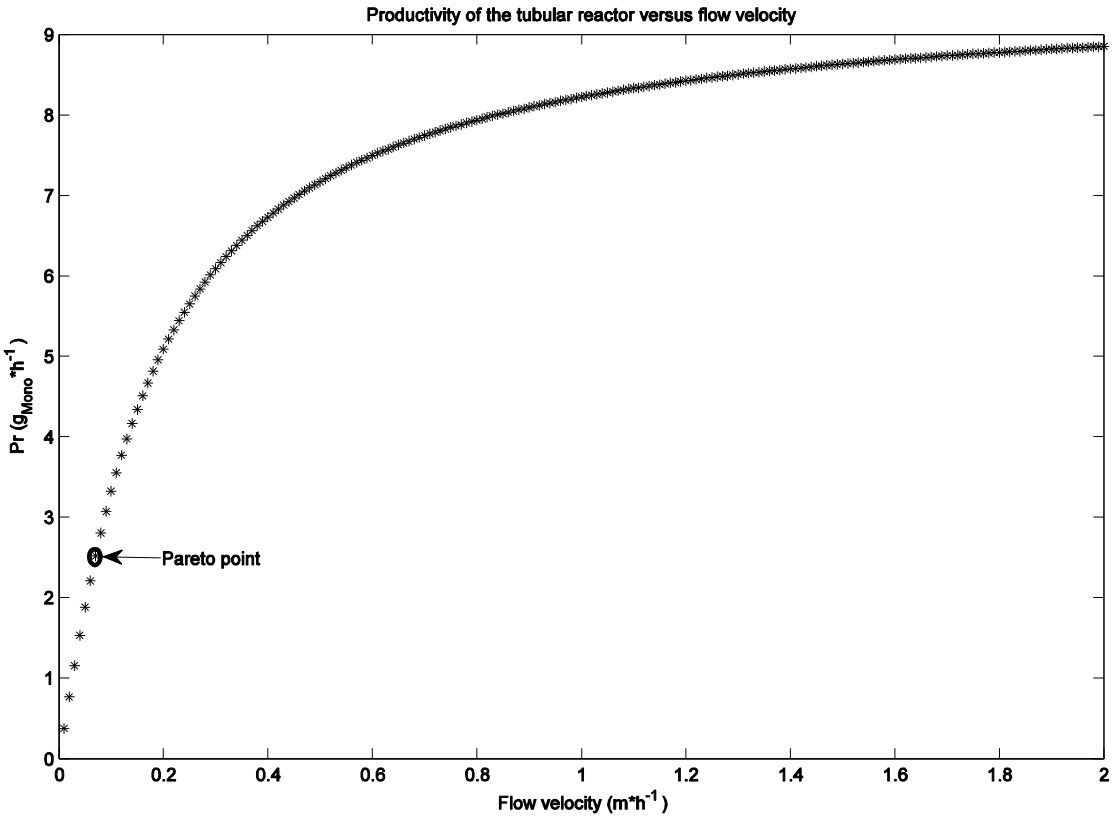

Figure 4.14. Influence of velocity on productivity for the tubular reactor, showing a logarithmic growth.

The chosen velocity, which was deterimend to be 0.06 $m \cdot h^{-1}$, was then used to simulate the entire tubular process. Process productivity was determined to be 0.0216 $g \cdot L^{-1} \cdot h^{-1}$ for a relatively low reaction time of 1.12 hours. Like previous cases, steady-state was reached after the five cycles. A complete compilation of the obtained data can be viewed in the

Case summary (paragraph **4.3.4**). Reaction profile for this optimisation can be seen in Figure 4.15.

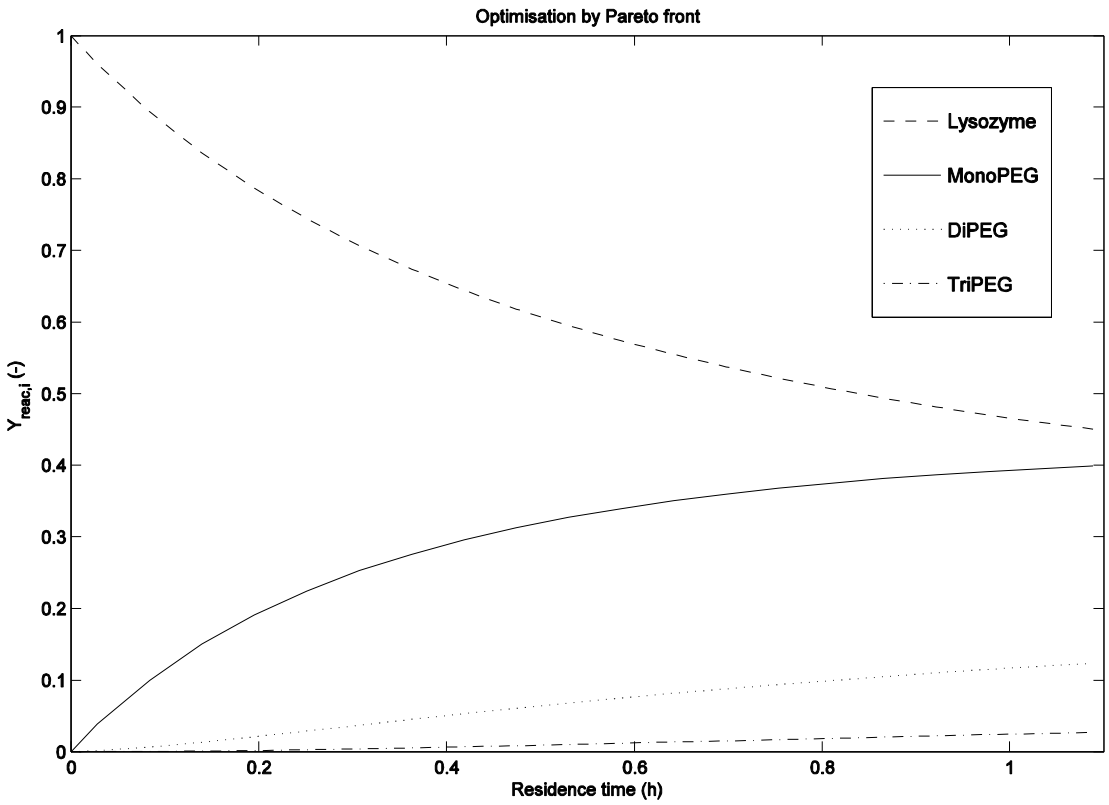

Figure 4.15. Illustration of reaction curve for the Pareto front case. Residence time for the components was 1.12 hours.

4.3.4 System performance analysis

In Table 4.3 below is a data summary collected from all cases made in the tubular process type.

Table 4.3. Data for three cases of tubular process investigated at steady-state of the recirculation process. I: waste yield below 10% of formed diPEGs. II: residence time constraint. III: Pareto front. Highlighted row was chosen to represent the tubular schematics.

**Case ran in flow velocity of 0.06 m·h^{-1}*

‡Residence time at 0th cycle

Case	t_{res}^{0} ‡ (h)	$Y_{reac,mono}$ (-)	$Y_{chrom,mono}$ (-)	$Y_{sys,mono}$ (-)	$Y_{sys,waste}$ (-)	Pr (g·h^{-1})
I	0.81	0.4557	0.9319	0.4246	0.1036	0.0217
II	5.00	0.4981	0.9872	0.4917	0.3222	0.0161
III*	1.12	0.4855	0.9533	0.4628	0.1457	0.0216

Before going in to study the phenomenon's generated by each case, it was thought that the most interesting part in this study would be to do a comparative analysis at cyclic steady-state.

Like noticed, the residence time (t_{res}^{0}) was chosen for the cases at 0th cycle since the recirculation will affect the systems differently depending on their reaction cutting points.

Studying the table above, one should first focus on the second column displaying the residence time at 0th cycle for each case. This column shows how the PEGylation process was affected by performance tests and should serve as an indication of the continuation of the process.

It is interesting to see how changes in the tube yield ($Y_{reac,mono}$) shows a great impact on the system by whole. At cyclic SS, **Case II** and **III** only differ by approximately 3%, which could be considered negligible. Comparing the mentioned cases to **Case I**, then there is an increase by 7-9% which is double the percentage unit. This is due to the early cutting point made in **Case I**. One would think that cutting early in the process and just recirculating the native protein would increase the yield, but at first it does not appear to be the case here. The reason for this probably lies in the calculations of the reactor yield since they were calculated in relation to starting concentration of lysozyme before the reaction. Taking the early cutting point and recirculation into consideration, this probably means that a larger portion of lysozyme is actually saved in **Case I** compared to the other cases in reality. This point is further strengthened by viewing the system waste yield, which is at almost 10% compared to 32% of **Case II**. However, in regards to mentioned type of tube yield calculation, **Case II** and **III** show a greater convertibility of native protein.

The productivity which fluctuates all the way from 0.0161 to 0.0217 $g \cdot h^{-1}$ when the yield (Y) is increased by 9%, from 0.46 to 0.50. Taking into consideration the system yield of **Case I** it is not acceptable compared to the other since it differs by 9% from **Case II** and 16% from **Case III**. Not a lot of monoPEGylated is produced and extracted. Even when comparing chromatography yields, **Case I** has a problem of fulfilling the purification requirements compared to **Case II** and **III**, which of course affects the system yield which is relatively low. Comparing **Case II** and **III** with each other reveals a higher process yield for **Case II**, a difference of about 4%. It should be noted that the yield from the chromatography column is at almost 0.99 which could be further pressed to down 0.95 to a more realistic value and thereby also increase the productivity. In comparison **Case III** shows a more realistic chromatography yield and seems to gain productivity by this, to approximately the same as **Case I** which is excellent.

Case conclusion

All over, **Case III** shows great qualities in comparison to the other two cases. Viewing the system waste yield, **Case I** and **III** show a huge difference in relation to **II**. A 55% reduction in waste formation is presented by **III** related to **II**. Residence time and productivity for **Case II** are too high and too low respectively. And the system yield is only slightly higher for **Case II** compared to **III**, and all over low for **I**. Taking the mentioned facts into consideration, **Case III** was chosen to represent the tubular reaction process.

4.4 Process performance comparison of batch vs tubular

Here the data for the two process schematics was brought together, see *Table 4.4*.

Table 4.4. Summary data for the two reactor processes. ***Case II*** *from the batch process and* ***Case III*** *from the tubular process.*

Process type	t_{res}^{0} (h)	$Y_{reac,mono}$ (−)	$Y_{chrom,mono}$ (−)	$Y_{sys,mono}$ (−)	$Y_{sys,waste}$ (−)	**Pr** ($g \cdot h^{-1}$)
Batch (Case II)	2.872	0.4378	0.9892	0.4331	0.2514	0.0126
Tube (Case III)	1.12	0.4855	0.9533	0.4628	0.1457	0.0216

First to notice is the residence time which the tube process is cut to almost a third of the batch which is a huge improvement. And thanks to the recirculation in the tube process, an increase can be seen in the reactor yield by almost 11%. The product system yield was approximately 7% higher for the tubular process. In reality this would probably be even more, since viewing the chromatographic yield of 99% being achieved by the batch case is more unrealistic than achieving 95% in the tubular process. Clearly the IEC column in the batch reactor process would experience a decrease of yield if the k-value was set lower. Consequently, the productivity would be reduced even more by such action.

Inspecting the system waste yield also shows a huge improvement. Going from batch to tubular schematics shows a decrease of waste by 42%. The main reason for this simply lies in the fact that the process is cut short compared to the batch reactor. No by-products have time to be formed and the recirculation allows for unreacted lysozyme to be saved and introduced to the PEGylation again.

By studying the productivity, an increase of about 71% could be made by implementing the tubular reactor system with recirculation. This is due to a couple of factors. First factor that affects the productivity is the formation of monoPEGylated proteins which is higher in the tubular process since more lysozyme is available in an excess of reactants. Another important factor that affects the productivity is the time for each component in the process. In the tubular case, dead time is negligible since tubular reactors can be run for a long time before any maintenance has to be performed. This is not the case for the batch reactor which experienced a total process time of 3.372, assuming 0.5 hour dead time.

Overall, the tubular reactor shows a much more flexible system. The batch reactor in itself is somewhat of a locked system since nothing can be done until a certain yield is reached. The tube reactor on the other hand combined with implemented recirculation system opens up a lot more options. Flow velocities, tube lengths and handling of recirculation stream in different ways offers better production of monoPEGs and more economic. The implementation of recirculation and the optimisation of various parts in the tubular process truly showed a greater improvement in comparison to the batch process.

4.5 General comments

Overall there is a lot to be said about the simulation and modelling in this project. The implementation of a tubular reactor was performed successfully, though the simulations were carried out in pulses, like a batch reactor in pulses through a column.

Besides the continuous processing benefit of the tubular reactor, it should be said that there are several other advantages by utilising it. Like previously mentioned in paragraph **2.2.1**, batch reactors are often preferred before any other type of reactor, mainly because of the strict pharmaceutical regulations. Nonetheless, if a batch is spoiled, then as obviously the whole batch is wasted. Components in a tubular reactor are much more defined compared to the batch reactor. And an optimised tube reactor will not have the same hold-up and for that reason, performance wise, not ruin as much biopharmaceutical protein if something goes wrong. Overall, the tube shows more adjustment flexibilities for optimisation.

4.5.1 Assumptions and options

As seen there are a lot of assumptions made for each part of the schematics in this project. Some of which are briefly discussed for each case in the subparagraphs below.

Salt filter

Only a simplistic salt filter model was used in this project simulation. Usually ultrafiltration is applied in the industry to filter salt dilutions. This model is assumes that no fouling takes place, which in reality affects productivity over time. Regarding the K_p value, the concentration out was assumed to be almost the same as the inlet flow (F_{in}) seen in Figure 3.2. It would have been more realistic to apply a value after an efficiency factor. If the protein concentration going out is more diluted than the reactor feed (higher K_p), the higher the permeate volume and thereby a higher filtration time according to Equations (27-28). Also, the flux is just an assumed value which could have some implications on the filtration time and area during sensitivity analysis. A larger flux, according to Equation (28), would imply less filtration time if the area and permeate are assumed to be the same. Another value which was assumed was the tubular reactor feed since it was not included in the report for the experimental setup.

Ion Exchange Chromatography

An assumption was made regarding the Peclét number which in turn can be found in Equation (18). As it is the only denominator in the equation and having a number set below 1, means that it could affect the axial dispersion coefficient immensely. In this simulation it was set to 0.5, but if set to 1 as in the case of Tegnér (2015), it is a reduction by 50%. However, even though it does reduce the D_{ax}, viewing it in a larger picture, it does not affect the overall elution since the D_{ax} already is such a low number.

Another assumption to be noticed are the column times for loading, washing, elution and regeneration. These are just set values which could be used to improve the column productivity.

Recirculation

When it comes to the recirculation in the system it was assumed a constant in flow to the reactor (F_{tot}) as seen in Figure 3.2. This could have various effects on the system since the inlet flow (F_{in}) would decrease thus reduce in the amount coming in to the reactor if the flow from the salt filter is high but not as concentrated. Ratio conversion of native protein would be more benefited, but a lot of productivity could be lost in the process. Therefore, it is of great importance how the flows are set to interact. It could also be performed in a way where the flow increases until a certain objective is met. Probably, in the case of yield and productivity,

it often is a matter of weighing the options to lean more to one of the two. Since this is a case of an expensive biopharmaceutical protein, one should strive more towards yield optimisation to recover the most biopharmaceuticals.

Tubular reactor
Assumed tube reactor specifications can be somewhat ambiguous, depending on how the person does the modelling. For the investigations done in this project the reactor radius was assumed to be 0.01 m. This affects the column length directly, because a small diameter means that a longer column is needed to cover the same amount of volume and vice versa. And this assumption could punish the process a lot more than it should. An increase in tube length also means an increase in flow velocity to keep the same hold-up time. In translation to power, this means more expensive pumps to counter the pressure drops received by longer tubes and larger energy consumption to pump the fluid. Same problem arises when assuming packing parameters of the column. Pressure drop is affected differently depending on the particle diameter and void.

Optimisation
As expected tolerances for the ODE-solvers and `fmincon` play an important role and should be fine-tuned accordingly. In this setup, the tolerances for the `fmincon` were set quite harshly, 10^{-12} for both `TolFun` and `TolX`. Such a tough tolerance affects the computational power for the simulation for something that may not converge. In cases, even when a high purity standard is required, such computational accuracy may not be needed at all. It is also worth noting that the values are the same which could cause a problem since they come in to play at different stages in the calculations. Nonetheless, it was realised at much later stage in the project that the values were set as they were in the beginning and were left that way. Not that they affected the simulation in any negative sense more than that it took a bit longer to simulate. But usually the optimisation stops long before tolerances of 10^{-12} are met.

5 Conclusions

A successful simulation and modelling of a tubular reactor was performed. Overall, more realistic data and features need to be implemented in the models to get truer picture of the process. However, the model can still give an indication what an implementation of a tubular reactor with recirculation would mean.

The tubular reactor showed promising potential for modification regarding optimisation. The ion exchange chromatography also displayed many favourable features to be enhanced; one of which was the salt gradient. An analysis showed that a higher k-value was preferred for a better and more efficient separation. The salt filter area was determined to be 2.06 cm^2 for a given k-value of 0.0838.

The tubular process showed a greater improvement in all aspects compared to the batch process. The model increased product yield by 11% (0.43 to 0.46), reduced waste yield by 42% (0.25 to 0.15), increased productivity by 71% (0.0126 to 0.0216 $g \cdot h^{-1}$) and this for a residence time being a third of the batch process.

In conclusion, a tubular reactor implemented with recirculation should be more simulated and experimented with. It shows great potential in proving to be more economical and better for increasing production of monoPEGylated proteins.

6 Further work

There are various things that could be considered for further development of this research.

The experiments carried out in order to gather data for the batch simulation could have been more thorough. Since only one experiment was carried out, statistical errors are possible and more work could be put into gathering reliable data.

Regarding the simulation and modelling in this project, it would be interesting to make the whole process continuous. First of all, instead of simulating pulses through the tubular reactor, it should be set up for a real time concentration profile along the reactor. The so called SMB would also be interesting to see being implemented. Not only achieve a better separation but for the main purpose of being able to complete the continuous process by its mechanisms. Of course, the salt filter would also have to be modified accordingly. It would also be interesting to try out another recirculation approach by for example trying to fuse together the streams rather than keeping tube reactor stream constant. This would also mean that a larger tubular reactor would be required.

When simulating the separation inside the IEC column, relatively simplistic mathematical models were used. Specifically, the dispersion model was used for this simulation. A more accurate method, however, is the General Rate Model which also takes particle diffusion into account. This could also be implemented for a better understanding of the IEC column separation and to attain a more realistic feature. In regards to striving for a more realistic modelling, fouling would be another component to be taken into consideration since it affects productivity. It would be of interest to see how the productivity is affected through time in relation to product earnings, when the minimally acceptable productivity is reached when the process is no longer profitable.

Using the Pareto front principle, other desired results could be more easily found like shown in one of the cases in this project. This principle could be further expanded for various different objectives. Optimisation in this process was made step-wise. That is, the optimal values were extracted from each and every step of the process and were then fed into the next step. It is, however, possible to create a large scale optimisation for the entire process, taking more parameters into account at one time. If the user has got one specific objective in mind, optimisation of the process could be more favourable. One way of bringing more information to the table would be for example to optimise the Pareto front with economic factors to generate a Pareto point instead of determining visually.

It would also be interesting to do a further sensitivity analysis on the loading, washing and elution times of the IEC column in relation to the salt filter while still considering the yield of the IEC and elution/washing buffers being used to further optimise the economical aspect in relation to total system yield and productivity.

As seen when the tubular reactor cases were compared, the k-value of the IEC column depended on incoming protein concentration. It would therefore be of interest to optimise the IEC process to respond for each specific concentration accordingly with appropriate salt gradient. By doing this, the elution would become more efficient and economical.

7 Reference list

1. Pfister D, Morbidelli M. Process for protein PEGylation. Journal of Controlled Release. 2014 February;: p. 134-149.

2. Hansen SK, Maiser B, Hubbuch J. Rapid quantification of protein-polyethylene glycol conjugates by multivariate evaluation of chromatographic data. Journal of Chromatography A. 2012 August 3; 1257: p. 41-47.

3. Bailon P, Won CY. Review: PEG-modified biopharmaceuticals. Expert Opinion on Drug Delivery. 2009 January; 6(1): p. 1-16.

4. Abuchowski A, McCoy JR, Palczuk NC, van Es T, Davis FF. Effect of Covalent Attachment of Polyethylene Glycol on Immunogenicity and Circulating Life of Bovine Liver Catalase. The Journal of Biological Chemistry. 1977 June 10; 252(11): p. 3582-3586.

5. Abuchowski A, Palczuk NC, van Es T, Davis FF. Alteration of Immunological Properties of Bovine Serum Albumin by Covalent Attachment of Polyethylene Glycol. The Journal of Biological Chemistry. 1977 June 10; 252(11): p. 3578-3581.

6. Pasut G, Veronese FM. Review: State of the art in PEGylation: The great versatility achieved after forty years of research. Journal of Controlled Release. 2012 July 20; 161(2): p. 461-472.

7. Roberts MJ, Bentley MD, Harris JM. Chemistry for peptide and protein PEGylation. Advanced Drug Delivery Reviews. 2002 January 22; 54: p. 459-476.

8. Fee CJ, Van Alstine JM. Prediction of the Viscosity Radius and the Size Exclusion Chromatography Behavior of PEGylated Proteins. Bioconjugate Chemistry. 2004 Nov-Dec; 15(6): p. 1304-1313.

9. Masier B, Kröner F, Dismer F, Brenner-Weiß G, Hubbuch J. Isoform separation and binding site determination of mono-PEGylated lysozyme with pH gradient chromatography. Journal of Chromatography A. 2012 December 14; 1268: p. 102-108.

10. Milton Harris J, Struck EC, Case MG, Paley MS, Yalpani M, Van Alstine JM, et al. Synthesis and characterization of poly(ethylene glycol) derivatives. Journal of Polymer Science: Polymer Chemistry Edition. 1984 February; 22(2): p. 341-352.

11. Harris JM, Chess RB. Effect of PEGylation on Pharmaceuticals. Nature Reviews Drug Discovery. 2003 March; 2: p. 214-221.

12. Roberts MJ, Bentley MD, Harris JM. Chemistry for peptide and protein PEGylation. Advanced Drug Delivery Reviews. 2002 January 22; 54: p. 459-476.

13. Yoshimoto N, Isakari Y, Itoh D, Yamamoto S. PEG chain length impacts yield of solid-phase protein PEGylation and efficiency of PEGylated protein separation by ion-exchange chromatography: insights of mechanistic models. Biotechnology Journal. 2013 July; 8(7): p. 801-810.

14. Kinstler O, Molineux G, Treuheit M, Ladd D, Gegg C. Mono-N-terminal poly(ethylene glycol)-protein conjugates. 2002 January; 54(4): p. 477-485.

15. Sprauer A, Mueller E, Christel J, Conze W, Noedinger V. http://www.chromatographyonline.com/. [Online].: Tosoh Bioscience GmbH; 2010 [cited 2015 08 10. Available from: http://www.chromatographyonline.com/characterization-studies-pegylated-lysozyme-using-tsk-gel-hplc-columns?id=&sk=&date=&pageID=2.

16. Tegnér F. Optimization of a PEGylation process: A combined reaction and separation with Size. H2 - Master's Degree. Lund: Lund University, Department of Chemical Engineering; 2015.

17. Gadamasetti K, Braish T, editors. Process Chemistry in the Pharmaceutical Industry, Volume 2: Challenges in an Ever Changing Climate. 1st ed.: CRC Press; 2007.

18. Fee CJ, Van Alstine JM. PEG-proteins: Reaction engineering and separation issues. Chemical Engineering Science. 2006 January; 61: p. 924-939.

19. Danielsson NÅ. Kemisk Reaktionsteknik A. Second edition ed. Lund; 2006.

20. Pan S, Zelger M, Hahn R, Jungbauer A. Continuous protein refolding in a tubular reactor. Chemical Engineering Science. 2014 September; 116: p. 763-772.

21. Bio-Rad. [Online]. [cited 2015 08 10. Available from: http://www.bio-rad.com/en-se/applications-technologies/liquid-chromatography-principles/ion-exchange-chromatography.

22. Pall Corporation. [Online]. [cited 2015 08 10. Available from: http://www.pall.com/main/laboratory/literature-library-details.page?id=42217.

23. Jian-gang L. Mathematical modeling of salt-gradient ion-exchange simulated moving bed chromatography for protein separations. Journal of Zhejiang University. Science. 2004 December; 5(12): p. 1613-1620.

24. Nilsson B. 1st order PDE: FVMdisc1st, 2nd order PDE: FVMdisc2nd, Boundary condition: FVMdiscBV.

25. LeVeque RJ. Finite Volume methods for hyperbolic problems: Cambridge University Press; 2002.

26. Andersson N. Parallell computing in model-based process engineering. 2014. Doctoral dissertation, Lund University.

27. Molek JM. Ultrafiltration of PEGylated Proteins. Doctoral thesis. The Pennsylvania State University, Chemical Engineering; 2008.

28. Ambrogelly A, Cutler C, Paporello B. Screening of Reducing Agents for the PEGylation of Recombinant Human IL-10. The Protein Journal. 2013 June; 32(5): p. 337-342.

8 Nomenclature

Table 8.1. Roman letters

Denotation	Unit	Definition
A	m^2	Area
c	$mole \cdot L^{-1}$	Concentration
c_i	$mole \cdot L^{-1}$	Concentration of component *i*
$c_{in,i}$	$mole \cdot L^{-1}$	Inlet concentration of component *i*
$c_{in,p}$	$mole \cdot L^{-1}$	Inlet concentration of protein
$c_{in,s}$	$mole \cdot L^{-1}$	Inlet concentration of salt
$c_{out,p}$	$mole \cdot L^{-1}$	Outlet concentration of protein
$c_{out,s}$	$mole \cdot L^{-1}$	Outlet concentration of salt
c_s	$mole \cdot L^{-1}$	Salt concentration
D_{ax}	$m^2 \cdot s^{-1}$	Axial dispersion coefficient
D_p	m	Particle diameter
D_s	-	Salt dilution factor
H_0	$m^3 \cdot mole^{-1}$	Experimental Henry's constant
H_i	$m^3 \cdot mole^{-1}$	Henry's constant
j	$L \cdot m^{-2} \cdot h^{-1}$	Flux
k_j	$dm^6 \cdot mole^{-2} \cdot s^{-1}$ $dm^{-3} \cdot mole^{-1} \cdot s^{-1}$	Kinetic reaction constant order *j*
k_{kin}	h^{-1}	Adsorption kinetic coefficient
K_p	-	Protein concentration factor
L	m	Column length
m	g	Mass
Pe	-	Peclét number
Pr	$g \cdot L^{-1} \cdot h^{-1}$	Productivity

q_i	$mole \cdot L^{-1}$	Stationary phase concentration of component *i*
$q_{max,i}$	$mole \cdot L^{-1}$	Maximum stationary phase concentration of component *i*
r_i	$mole \cdot L^{-1} \cdot s^{-1}$	Reaction rate for component *i*
r_j	$mole \cdot L^{-1} \cdot s^{-1}$	Reaction rate order *j*
t	h	Time
$\boldsymbol{t_{res}^{0}}$	h	Residence time for 0th cycle
t_{filt}	h	Filtration time
V_{feed}	m^3	Feed volume
V_{perm}	m^3	Permeate volume
V_{ret}	m^3	Retention volume
V_{sf}	m^3	Salt feed volume
Y	$mole \cdot mole^{-1}$	Yield
z	m	Tube/column length

Table 8.2. Greek letters

Symbol	Unit	Definition
β	-	Adsorption parameter
ϵ	-	Total column porosity
ϵ_c	-	Bed porosity, fluid **outside** packing
ϵ_p	-	Packing porosity, fluid **inside** particles
θ	h	Residence time
υ	$m \cdot s^{-1}$	Flow velocity

Table 8.3. Subscripts

Symbol	Definition
CBH	Sodium cyanoborohydride
cyc	Cycles
di	Di-PEGylated lysozyme
i	Component
j	Order
Lys	Lysozyme
mono	MonoPEGylated lysozyme
reac	Reactor
sys	System
tri	Tri-PEGylated lysozyme